# SUPERCONDUCTIVITY IN d- AND f-BAND METALS

Second Rochester Conference

Edited by D. H. Douglass

University of Rochester
Rochester, New York

1976

Plenum Press · New York and London

GAP ANISOTROPY AND $T_c$ ENHANCEMENT: GENERAL THEORY, AND CALCULATIONS FOR Nb, USING FERMI SURFACE HARMONICS

W. H. Butler

Oak Ridge National Laboratory*

Oak Ridge, Tennessee 37830

and

P. B. Allen †

State University of New York

Stony Brook, New York 11794

ABSTRACT

A general theory is given of the anisotropy of the energy gap and the resulting transition temperature ($T_c$) enhancement of pure superconductors. The frequency dependence of the gap $\Delta(k,\omega)$ is approximated by the two square well form of McMillan, but otherwise an exact algebraic solution of the strong-coupling Eliashberg equations is given, valid for arbitrarily large anisotropy. In the limit of weak anisotropy a simple perturbative formula is also derived. The method of solution relies on the use of expansion functions called Fermi surface harmonics (FSH's) which are velocity polynomials orthonormalized on the Fermi surface. Methods for explicit construction of these functions are described. As an application of these techniques the mass enhancement and gap anisotropy are calculated for Nb, in an approximation which includes all electronic anisotropy but neglects the contribution to the anisotropy which arises from phonons. The rms gap anisotropy in this model is 6% which is not inconsistent with most of the current experimental data. The resulting $T_c$ enhancement is predicted to be 0.7% or .06°K.

* Research supported by ERDA under contract with Union Carbide Corp.
† Supported in part by NSF Grant No. DMR 73-07578A01

## I. INTRODUCTION

Microscopic theory[1,2,3] gives a four-dimensional integral equation for the energy gap $\Delta(k,\omega)$. Experiments such as tunneling[4] are especially good at probing the dependence of $\Delta$ on the external frequency $\omega$ (given by voltage eV in tunneling), and can also yield information about the variation of $\Delta$ as $\underset{\sim}{k}$ varies on the Fermi surface. To make theoretical calculations possible it is helpful to approximate the four dimensional integral equation by a lower dimensional equation. The usual procedure is to replace $\Delta(k,\omega)$ by an average value $\Delta_o(\omega)$

$$\Delta_o(\omega) = \frac{1}{\nu} \sum_{\underset{\sim}{k}} \Delta(k,\omega)\delta(\varepsilon_k) \tag{1}$$

$$\nu = \sum_{\underset{\sim}{k}} \delta(\varepsilon_k) \tag{2}$$

which is the isotropic average of $\Delta(k,\omega)$ over the Fermi surface. In these equations k is shorthand for wavevector $\underset{\sim}{k}$, band index n, and spin $\underset{\sim}{\sigma}$. Thus the density of states at the Fermi surface, $\nu$, is for both spin orientations.

Most of our current understanding of the interactions and thus transition temperature ($T_c$) of superconductors derives from such an isotropically averaged theory. In particular, McMillan's inversion program[4] and $T_c$ equation[5] both make this approximation. An excellent justification for the isotropic approximation exists in dirty superconductors where impurity scattering causes the actual gap to be isotropically averaged[6]. However, it has long been known that in situations where $\Delta(k,\omega)$ has a significant variation on the Fermi surface, $T_c$ is higher than in the dirty or isotropic limit. The earliest theoretical model of this was the two band model proposed by Suhl et al.[7] and by Moskalenko[8], in which the Fermi surface is presumed to have two unrelated pieces and the gap is allowed to take a different value on each piece. The case of more general anisotropy has been treated in the weak coupling and weak anisotropy approximation by many authors, perhaps first by Pokrovskii[9]. The exactly soluble model of a separable potential was introduced and solved as a function of impurity scattering by Markowitz and Kadanoff[10], Tsuneto[11], and Caroli et al.[12]. Numerous other authors have extended this theory[13-15].

Motivated by the conjecture that anisotropy enhancement might contribute significantly to the $T_c$ of high temperature superconductors, we have reexamined the theory of anisotropic superconductors without making the weak coupling or weak anisotropy approximations. Similar work has been reported by other authors[16,17] but we believe to have found an approach which is particularly simple and general, and well adapted for both analytic arguments and numerical calculations. In this paper we present detailed discussion of a calculation of the gap anisotropy and $T_c$ enhancement of pure niobium. Other problems such as impurity effects[18], critical fields, and normal state transport properties[19] can be profitably discussed in the same language, and such work will be published at a later date. The calculations presented here take full account of the anisotropy which derives from the energy bands and Fermi surface, but neglects anisotropy which arises from the phonon dispersion. We hope to present more complete calculations including phonon-induced anisotropy at a later date.



The new mathematical method which enables us to find simple solutions to anisotropic problems is the technique of Fermi Surface Harmonics[20] (FSH's). The general properties of these functions are discussed in a recent paper[20]. In brief, the idea is that an integral equation such as the Eliashberg equation will become a simple matrix equation if we expand the kernel and the gap in a basis set which is orthonormal on the actual Fermi surface under consideration. Such functions are labeled $F_J(k)$, and must be constructed separately for each metal. The appropriate orthonormality relation is

$$\frac{1}{\nu} \sum_{\underset{\sim}{k}} F_J(k)F_{J'}(k)\delta(\varepsilon_k) = \delta_{JJ'} \ . \tag{3}$$

There are five additional properties which it would be desirable for $F_J(k)$ to have:

(i) $F_J(k)$ should be cell periodic in k-space (that is $F_J(\underset{\sim}{k}+\underset{\sim}{G}) = F_J(\underset{\sim}{k})$ for all reciprocal lattice vectors $\underset{\sim}{G}$). This is accomplished by choosing $F_J$ to depend only on the velocity $\underset{\sim}{v}_k = \underset{\sim}{\nabla}_k\varepsilon_k$, where $\varepsilon_k$ is the band-theoretic electron dispersion relation.

(ii) The isotropic case should have a simple representation. This is accomplished by choosing the first function $F_o = 1$.

(iii) The point symmetry of the crystal should be fully exploited This is done by requiring $F_J$ to transform as basis functions for irreducible representations of the point group.

(iv) The functions $F_J(k)$ should reduce to spherical harmonics $Y_{\ell m}(\hat{k})$ if the Fermi surface is a sphere. This is accomplished by choosing $F_J(k)$ to be polynomials in $(v_{kx}, v_{ky}, v_{kz})$. In the spherical case, $\underset{\sim}{v}_k$ is proportional to $\hat{k}$ and $Y_{\ell m}$ is a polynomial in $k_x$, $k_y$, $k_z$.

(v) The gap $\Delta(k,\omega)$ and other properties should have rapidly convergent expansions in FSH's. This is not possible to guarantee a priori, and will be tested in this paper for Nb.

The plan of this paper is as follows. In Section II the Eliashberg equations are written in the FSH representation, and a $T_c$ equation is found in the two-square well approximation. In Section III, perturbation theory is used to simplify the $T_c$ equation in the limit of weak anisotropy. The relation between $T_c$ enhancement and rms gap anisotropy is given for strong-coupled superconductors for the first time. In Section IV the equations of Section II are examined in the two-band approximation, and the $T_c$ equation of Suhl et al[7] is derived with strong-coupling corrections included. In Section V we enumerate the low order Fermi surface harmonics for Nb and explain how they are constructed. In Section VI we show how the quantities entering the equations of Section II can be obtained from energy band calculations. In Section VII the completeness of the FSH's tested for Nb by explicit calculations of the expansion coefficients of various components of the density matrix. Typically 95% completeness has been achieved with an average of six functions on each of the three sheets of Fermi surface. In Section VIII the calculated coefficients of the anisotropic gap and mass enhancement are presented and discussed and compared with experiment.

## II. DERIVATION OF $T_c$ EQUATION

Our starting point is the Eliashberg theory[2,3] for the frequency-dependent complex gap $\Delta(\omega)$ as a function of the real external frequency $\omega$. The equations are given by McMillan[5] as eq. (2). Our treatment will be exactly parallel to McMillan's except that we generalize to the case of an anisotropic gap

$$\Delta(k,\omega) = \sum_J \Delta_J(\omega) F_J(k) \tag{4}$$

and we also make minor modifications to give an improved[21] prefactor, $\omega_{log}$, in the final $T_c$ equation. The anisotropic equations are eqs. (37-39) of ref. 20

$$\begin{aligned}\phi_J(\omega) &= \sum_{J'} [\delta_{JJ'} + \Lambda_{JJ'}(\omega)]\Delta_{J'}(\omega) \\ &= -\sum_{J'} \int_{-\infty}^{\infty} \frac{d\omega'}{\omega'} \int_0^{\infty} d\Omega \alpha_{JJ'}{}^2F(\Omega)\,\mathrm{Re}[\Delta_{J'}(\omega')]K(\omega,\omega',\Omega) \\ &\quad - \sum_J \mu_{JJ'} \int_0^{\omega_p} \frac{d\omega'}{\omega'} \mathrm{Re}[\Delta_{J'}(\omega')]\tanh\frac{\beta\omega'}{2} \quad .\end{aligned} \tag{5}$$



The pair field $\phi$ is equal to $Z\Delta$ in the isotropic limit, where Z is $1 + \Lambda_{00}(\omega)$ and is called the renormalization function. The anisotropic theory gives a slightly more complicated relation, and we introduce a tensor $\Lambda_{JJ'}(\omega)$ defined by

$$\omega\Lambda_{JJ'}(\omega) = -\sum_{J''} C_{JJ'J''} \int_{-\infty}^{\infty} d\omega' \int_0^{\infty} d\Omega \alpha_{J''0}{}^2F(\Omega)K(\omega,\omega',\Omega) \tag{6}$$

where $C_{JJ'J''}$ is a Clebsh-Gordan coefficient defined in ref. 20. The interaction parameters $\alpha^2_{JJ'}F(\Omega)$ and $\mu_{JJ'}$ are matrix elements in the FSH basis of the phonon and electron interactions. An explicit formula for $\alpha_{JJ'}{}^2F(\Omega)$ is given in eq. (33) of ref. 20. For our purposes, the most important parameters are the integrated strength $\lambda_{JJ'}$,

$$\begin{aligned}\lambda_{JJ'} &= 2\int_0^{\infty} \frac{d\Omega}{\Omega} \alpha_{JJ'}{}^2F(\Omega) \\ &= \frac{1}{\nu} \sum_{kk'i} (|M^i_{kk'}|^2/\omega^i_{k-k'}) F_J(k)F_{J'}(k')\delta(\varepsilon_k)\delta(\varepsilon_{k'})\end{aligned} \tag{7}$$

and the zero frequency, zero temperature renormalization parameter $\Lambda_{JJ'}$

$$\begin{aligned}\Lambda_{JJ'} &= \sum_{J''} C_{JJ'J''} \lambda_{J''0} \\ &= \frac{1}{\nu} \sum_{kk'i} (|M^i_{kk'}|^2/\omega^i_{k-k'}) F_J(k)F_{J'}(k)\delta(\varepsilon_k)\delta(\varepsilon_{k'})\end{aligned} \tag{8}$$

In these equations $M_{kk'}$ is the electron-phonon matrix element, $\omega^i_{k-k'}$ is the phonon frequency, and i is the phonon polarization index. The difference between $\lambda_{JJ'}$ and $\Lambda_{JJ'}$ is that both FSH's have the same argument, k, in eq. (8), whereas in (7) the arguments are different. The Coulomb coupling matrix $\mu_{JJ'}$ is defined as

$$\mu_{JJ'} = \frac{1}{\nu} \sum_{kk'} V_{kk'} F_J(k)F_{J'}(k')\delta(\varepsilon_k)\delta(\varepsilon_{k'}) \tag{9}$$

where $V_{kk'}$ is the matrix element of the (screened and vertex-corrected) Coulomb potential which scatters a spin up electron from k to k' and

a spin down electron from -k to -k'. The plasma frequency $\omega_{p\ell}$ is the natural cutoff of the Coulomb interaction.

The equations of an isotropic or dirty superconductor are obtained from (5) and (6) by assuming that $\alpha^2_{JJ'}F(\Omega)$ is diagonal in JJ'. This guarantees that $\Lambda_{JJ'}(\omega)$ is diagonal because of the relation[20] $C_{JJ'0} = \delta_{JJ'}$. In this approximation equation (5) becomes a set of uncoupled equations, one for each value of J, with the J=0 equation being eq. (2) of McMillan's paper[5]. The usual parameters $\lambda,\mu$ and $\alpha^2F$ are identified $\lambda_{oo}$, $\mu_{oo}$, $\alpha^2_{oo}F$. The effect of impurities is to introduce a strong repulsive term which will drastically reduce or eliminate all coupling constants except for the J=0, J'=0 component where the impurity term is absent in accordance with Anderson's theorem[6].

In an attempt to solve these equations, we now follow McMillan[5] in making the two-square-well approximation,

$$\Delta_J(\omega) = \begin{cases} \Delta_J(0) & \text{if} \quad |\omega| < \omega_{ph} \\ \Delta_J(\infty) & \text{if} \quad \omega_{ph} < |\omega| < \omega_{p\ell} \\ 0 & \text{otherwise} \end{cases}$$

$$\Lambda_{JJ'}(\omega) = \begin{cases} \Lambda_{JJ'} & \text{if} \quad |\omega| < \omega_{ph} \\ 0 & \text{otherwise} \end{cases} \qquad (10)$$

where $\omega_{ph}$ is the maximum phonon energy and $\Delta J(0)$, $\Delta_J(\infty)$ are assumed real. The kernel $K(\omega,\omega',\Omega)$ of eqs. (5) and (6) is given by

$$K(\omega,\omega',\Omega) = \frac{f(\omega') + N(\Omega)}{\omega-\omega' + \Omega} + \frac{f(-\omega') + N(\Omega)}{\omega-\omega' - \Omega} . \qquad (11)$$

Observing that $|\Omega|$ is confined to frequencies less than $\omega_{ph}$, we make the approximation that K is zero unless both $|\omega|$ and $|\omega'|$ are less than $\omega_{ph}$. Then using these approximations, we evaluate eq. (5) at $\omega=0$ and $\omega=\infty$ (actually $\omega \lesssim \omega_{p\ell}$ is meant rather than $\infty$) to get self-consistent equations for $\Delta_J(0)$ and $\Delta_J(\infty)$,



$$\sum_{J'}(\delta_{JJ'} + \Lambda_{JJ'})\Delta_{J'}(0) =$$

$$\sum_{J'}(A_{JJ'} - \mu_{JJ'} \ln(1.13\beta\omega_{ph}))\,\Delta_{J'}(0)$$

$$- \sum_{J'} \mu_{JJ'} \ln(\omega_{p\ell}/\omega_{ph})\Delta_{J'}(\infty) \qquad (12)$$

$$\Delta_J(\infty) = -\sum_{J'} \mu_{JJ'} \ln(1.13\beta\omega_{ph})\Delta_{J'}(0)$$

$$- \sum_{J'} \mu_{JJ'} \ln(\omega_{p\ell}/\omega_{ph})\Delta_{J'}(\infty) . \qquad (13)$$

Here $A_{JJ'}$ is defined as

$$A_{JJ'} = \int_0^\infty d\Omega\alpha^2_{JJ'}F(\Omega) \int_{-\omega_{ph}}^{\omega_{ph}} d\omega' \; K(0,\omega',\Omega)/\omega' \qquad (14)$$

$$\gtrsim 2 \int_0^\infty \frac{d\Omega}{\Omega} \alpha^2_{JJ'}F(\Omega) \ln(1.13\beta\Omega) \qquad (15)$$

$$\equiv \lambda_{JJ'} \ln 1.13\beta\omega_{log} + \delta\lambda_{JJ'} \qquad (16)$$

and the logarithmic average frequency, $\omega_{log}$, is defined as in ref. 21

$$\ln(\omega_{log}) \equiv \frac{2}{\lambda} \int_0^\infty \frac{d\Omega}{\Omega} \; \alpha^2F(\Omega) \; \ln\Omega \qquad (17)$$

$$\delta\lambda_{JJ'} \equiv 2 \int_0^\infty \frac{d\Omega}{\Omega} \; \alpha_{JJ'}{}^2F(\Omega) \ln(\Omega/\omega_{log}) \qquad (18)$$

The isotropic component $\delta\lambda_{oo}$ vanishes by the definition (17). In going from (14) to (15) we have extracted the leading term in weak coupling (i.e. treating $\beta\Omega$ as large). It has been found that treating corrections to (15) of higher order in $(\beta\Omega)^{-1}$ leads to incorrect conclusions. The problem is that the two square well model fails if the coupling is very strong[22]; $T_c$ has been shown[21] both experimentally and theoretically to increase more strongly as $\lambda$ increases than is

allowed in this model. However, it has also been shown[21] that this model is highly accurate for materials with $\lambda < 1.5$. Therefore in the present paper, we work in the two square-well approximation.

Equations (12), (13), and (16) are now easily solved to find $T_c$. First we solve (13) for $\Delta(\infty)$,

$$\Delta_J(\infty) = -\sum_{J'} \ln(1.13\beta\omega_{ph})\mu^*_{JJ'}\Delta_{J'}(0) \tag{19}$$

where the matrix $\underset{\sim}{\mu}^*$ is related to $\underset{\sim}{\mu}$ by

$$\underset{\sim}{\mu}^* = (\underset{\sim}{1} + \underset{\sim}{\mu} \ln(\omega_{p\ell}/\omega_{ph}))^{-1}\underset{\sim}{\mu}. \tag{20}$$

Then we use (18) to eliminate $\Delta(\infty)$ from (12), giving

$$\rho(\underset{\sim}{1} + \underset{\sim}{\Lambda} - \delta\underset{\sim}{\lambda} + \delta\underset{\sim}{\mu}^*) \cdot \underset{\sim}{\Delta}(0) = (\underset{\sim}{\lambda}-\underset{\sim}{\mu}^*)\cdot\underset{\sim}{\Delta}(0) \tag{21}$$

where we have defined

$$\delta\underset{\sim}{\mu}^* = \ln(\omega_{ph}/\omega_{log})\underset{\sim}{\mu}^* \tag{22}$$

$$1/\rho = \ln(1.13\beta\omega_{log}) \tag{23}$$

Equation (21) is the final equation which determines the anisotropic zero frequency gap $\Delta(k,0)$ at $T = T_c$. This equation has non-trivial solutions $\Delta \neq 0$ only for discrete eigenvalues $\rho$. The actual transition temperature corresponds to the maximum eigenvalue $\rho$ which we denote $\lambda_{eff}$.

$$T_c = 1.13\omega_{log}\, e^{-1/\lambda_{eff}} \tag{24}$$

$$\lambda_{eff} = \text{Max. Eigenvalue of } (\underset{\sim}{1} + \underset{\sim}{\Lambda} - \delta\underset{\sim}{\lambda} + \delta\underset{\sim}{\mu}^*)^{-1}(\underset{\sim}{\lambda}-\underset{\sim}{\mu}^*) \tag{25}$$



Equations (24) and (25) are the $T_c$ equation we have been seeking. They take full account of strong coupling corrections and are valid for arbitrarily large anisotropy. However, the use of the two square-well model limits their validity to materials with $\lambda \lesssim 1.5$. Furthermore, detailed numerical solutions[21] in the isotropic approximation suggest that the prefactor 1.13 should be replaced by 1/1.20.

In terms of practical applications, it may appear disturbing that eq. (25) involves a large number of microscopic coupling constants, namely five matrices $\underset{\sim}{\lambda}$, $\underset{\sim}{\mu}^*$, $\underset{\sim}{\Lambda}$, $\delta\underset{\sim}{\lambda}$, and $\delta\underset{\sim}{\mu}^*$. However, things are not as complicated as they may seem. For example, the matrix $\delta\underset{\sim}{\mu}^*$ is proportional to $\underset{\sim}{\mu}^*$. The upper left hand element, $\mu^*_{oo} = \mu^*$ is of order 0.1, and the other elements in all likelihood are considerably smaller (and therefore negligible). The matrix $\delta\underset{\sim}{\lambda}$ has a vanishing upper left element. The other elements are non-vanishing only to the extent that the shape of $\alpha^2_{JJ'}F(\Omega)$ differs from the shape of $\alpha^2F(\Omega)$. Each element of $\delta\underset{\sim}{\lambda}$ is small compared to the corresponding element of $\underset{\sim}{\lambda}$ and therefore, in all likelihood, also negligible. The Matrix $\underset{\sim}{\Lambda}$ has elements which can all be expressed in terms of the elements of the matrix $\underset{\sim}{\Lambda}$ and the Clebsh-Gordan coefficients. These can be calculated if a reliable Fermi surface is known, and most of the important Clebsh-Gordan coefficients are either 0 or 1. Thus to a good approximation we seek the maximum eigenvalue of $(\underset{\sim}{1} + \underset{\sim}{\Lambda})^{-1}(\underset{\sim}{\lambda} - \mu^*\,\delta_{J0}\delta_{J0'})$ which involves only one matrix of coupling constants $\lambda_{JJ'}$. Group theory has been used in constructing the functions $F_J(k)$. This has the helpful consequence that all five matrices are block-diagonal, i.e. the only non-vanishing off-diagonal elements are those connecting functions which belong to the same row of the same irreducible representation. In cubic symmetry, there are ten irreducible representations, and a total of twenty rows. Thus the matrix $(\underset{\sim}{1} + \underset{\sim}{\Lambda} - \delta\underset{\sim}{\lambda} + \delta\underset{\sim}{\mu}^*)^{-1}(\underset{\sim}{\lambda} - \underset{\sim}{\mu}^*)$ consists of twenty submatrices, i.e. a $\Gamma_1$ submatrix which determines the s-wave transition temperature, three (identical appearing) $\Gamma_{15}$ submatrices corresponding to the three rows of the $\Gamma_{15}$ representation which determine the p-wave transition temperature, and so forth. Ordinarily we expect the s-wave transition temperature to be highest, although it has been suggested[23] that because $\mu^*$ may be small in the p-wave channel, some metals with small values of $\lambda$ may have p-wave instabilities at very low temperatures. At any rate, the problem of determining the s-wave transition temperature involves examining only the $\Gamma_1$ submatrix, which in favorable cases can probably be accurately represented with a fairly small number of terms.

Finally it is important to note that the matrices $\underset{\sim}{\lambda}$ and $\underset{\sim}{\Lambda}$ describe material properties relevant in other problems besides superconductivity. For example, the low temperature normal state specific heat is enhanced by $1 + \lambda_{oo} = 1 + \lambda$. The high temperature electrical resistance is determined by the p-wave submatrix[20] of $\underset{\sim}{\Lambda}-\underset{\sim}{\lambda}$. Thus the zoo of new coefficients introduced here is by no means so large and arbitrary as may at first sight appear.

## III. THE LIMIT OF WEAK ANISOTROPY

In the previous section we have derived equations for the anisotropic gap parameter and the transition temperature. We repeat here a simplified version of these equation

$$\lambda_{eff}(\underset{\sim}{1} + \underset{\sim}{\Lambda}) \cdot \underset{\sim}{\Delta} = (\underset{\sim}{\lambda} - \underset{\sim}{\mu}^*)\cdot\underset{\sim}{\Delta} \tag{26}$$

$$T_c = (\omega_{log}/1.2)\ \exp\ (-1/\lambda_{eff}). \tag{27}$$

We have neglected the small matrices $\delta\underset{\sim}{\lambda}$, $\delta\underset{\sim}{\mu}^*$, and introduced an empirical adjustment of the prefactor. These equations have the same form in any orthonormal basis set. In particular, Entel and Peter[17] have recently presented these equations, working in the "locally constant" representation - that is, their orthonormal functions are constants in isolated (i.e. non-overlapping) regions and zero elsewhere. Clearly such functions can be normalized so as to satisfy the condition (1). However, the FSH basis set has several advantages over that of Entel and Peter, one being that the equations take a simple form if the anisotropy is weak. Specifically, the matrices $\underset{\sim}{\Lambda}$, $\underset{\sim}{\lambda}$, and $\underset{\sim}{\mu}^*$ become nearly diagonal, and the maximum eigenvalue is closely approxiamted by the upper left hand term, i.e.

$$\lambda_{eff}(iso)\ (1 + \lambda) = \lambda - \mu^*$$

$$T_c(iso) = (\omega_{log}/1.2)\ \exp(-(1 + \lambda)/(\lambda - \mu^*)). \tag{28}$$

Apart from small adjustments, this is the familiar McMillan equation[5]. If the anisotropy is not too strong, it is a simple matter to find corrections to the isotropic equation by perturbation theory, and also to find the gap anisotropy perturbatively. These tasks would be harder in alternative basis sets such as that of Entel and Peter.

Equation (26) allows us to calculate the gap anisotropy only at $T = T_c$ where $\Delta$ is vanishingly small. At lower temperatures where $\Delta$ is no longer negligibly small, non-linear terms occur in the original integral equation which determine the magnitude of $\Delta$. The non-linearality consists of putting the J' component of $\mathrm{Re}[\Delta/\sqrt{\omega'^2+\Delta^2}]$ in place of $\mathrm{Re}[\Delta_{J'}]/\omega'$ in eq. (5). If we make the approximation

$$[\Delta/\sqrt{\omega'^2+\Delta^2}]_{J'} \approx \Delta_{J'}/\sqrt{\omega'^2+\Delta_o^2} \tag{29}$$



then the gap equation is soluble by methods similar to those we used to find $T_c$. Within this approximation we find that the relative anisotropy (i.e. $\Delta_J/\Delta_o$) is independent of temperature. Thus it is sufficient to solve the linear equation (21) or (26) to learn the relative anisotropy at all temperatures. This approximation was first described by Anderson and Morel[24] and Pokrovskii[9], and has been tested by Leavens and Carbotte[25] who found that the corrections were small, using an iterative procedure. In the weak anisotropy approximation, we seek solutions of the form

$$\Delta(k,o) = \Delta_o[1 + \sum_{J\neq 0} (\Delta_J/\Delta_o)F_J(k)] \tag{30}$$

$$\lambda_{eff} = (\lambda - \mu^*)/(1 + \lambda) + \delta\lambda_{eff} \tag{31}$$

where $\Delta_J$ and $\delta\lambda_{eff}$ are assumed small compared with $\Delta_o$ or $\lambda_{eff}(iso)$ respectively. In the weak coupling limit where $\underset{\sim}{\Lambda}$ is neglected relative to $\underset{\sim}{1}$, eq. (26) is a Hermitean eigenvalue problem, and the Rayleigh-Ritz perturbation series for ground state wavefunction and energy in quantum mechanics. The results in lowest order are:

$$\left(\frac{\Delta_J}{\Delta_o}\right) = \frac{(\underset{\sim}{\lambda}-\underset{\sim}{\mu}^*)_{0J}}{(\underset{\sim}{\lambda}-\underset{\sim}{\mu}^*) - (\underset{\sim}{\lambda}-\underset{\sim}{\mu}^*)_{JJ}} \approx \frac{\lambda_{0J}}{\lambda-\mu^*}$$

($J \neq 0$, weak coupling)

$$\delta\lambda_{eff} = \sum_{J\neq 0} \frac{(\underset{\sim}{\lambda}-\underset{\sim}{\mu}^*)_{0J}^2}{(\underset{\sim}{\lambda}-\underset{\sim}{\mu}^*)_{oo} - (\underset{\sim}{\lambda}-\underset{\sim}{\mu}^*)_{JJ}} \approx \sum_{J\neq 0} \frac{\lambda_{0J}^2}{\lambda-\mu^*} \tag{32}$$

(weak coupling)

The approximate forms on the right invoke the assumption that $\underset{\sim}{\mu}^*$ has only an upper left term $\mu^*$ which is non-zero. The weak anisotropy approximation assumes only that off-diagonal elements of $\underset{\sim}{\lambda}$ are small. It is probably reasonable to assume that the diagonal elements for $J\neq 0$ are also small, and thus to omit $\lambda_{JJ}$ from the denominators as a higher order correction. This approximation has also been introduced on the right in eq. (32). We introduce the root-mean-square (rms) fractional anisotropy $\alpha$, defined as

$$\alpha \equiv \sqrt{\langle\Delta^2\rangle - \langle\Delta\rangle^2}\ /\langle\Delta\rangle$$

$$= \left[\sum_{J\neq 0} (\Delta_J/\Delta_o)^2\right]^{1/2} \tag{33}$$

where the last expression is a general formula derived from eq. (1), and the angular brackets < > are used to denote a Fermi surface average,

$$\langle P_k\rangle \equiv \nu^{-1} \sum_k P_k \delta(\varepsilon_k). \tag{34}$$

In the weak coupling approximation (where $\lambda_{eff} = \lambda - \mu^*$) we find from (32) and (33)

$$\alpha^2 = \delta\lambda_{eff}/\lambda_{eff} = \lambda_{eff}\ \delta T_c/T_c(iso) \tag{35}$$

This result has been derived many times, usually within the factorizable interaction model[10-12], and is derived here for weak coupling and weak anisotropy (but with no restriction as to the form of the anisotropic interactions). This result shows that the fractional $T_c$ enhancement due to anisotropy scales as the square of the rms gap anisotropy. Thus a 10% gap anisotropy (as is commonly seen by tunneling in s-p metals) gives a $T_c$ enhancement of order 1%. The actual size of the fractional $T_c$ enhancement is larger for low $T_c$ materials where $\lambda_{eff}$ is small. For example, the alloy data of Farrell et al[26] for Zn, a weak coupling material ($\lambda_{eff} \approx 0.20$), indicate a $T_c$ enhancement of 20%; eq. (35) then implies a 20% rms gap anisotropy.

Let us now derive the strong coupling corrections to eqs. (32) and (35). If we made the assumption that the renormalization matrix $(1 + \underset{\sim}{\Lambda})$ were diagonal and equal to $(1 + \lambda)\underset{\sim}{1}$ (as it is in the isotropic limit) then the derivation would be simple. Each term $\lambda_{JJ'}$ and $\mu^*_{JJ'}$ of eq. (32) would simply be renormalized (i.e. reduced) by a factor $(1 + \lambda)$ leaving the gap anisotropy $\Delta_J/\Delta_o$ unaffected, and reducing $\delta\lambda_{eff}$ by $(1 + \lambda)$. The form of eq. (35) would be unaltered (because the formula for $\lambda_{eff}$ is altered to $(\lambda-\mu^*)/(1+\lambda)$. However, not all of these conclusions are correct, because the renormalization $\underset{\sim}{\Lambda}$ has anisotropic corrections which need to be handled in the same order of approximation as the anisotropic corrections to $\underset{\sim}{\lambda}$. The derivations are somewhat tricky and are given below, but the final results are gratifyingly simple:



$$\frac{\Delta_J}{\Delta_o} = \left(\frac{1+\mu^*}{1+\lambda}\right) \frac{\lambda_{0J}-\mu^*_{0J}(1+\lambda)/(1+\mu^*)}{(\lambda-\mu^*) - (\lambda-\mu^*)_{JJ}} \approx \left(\frac{1+\mu^*}{1+\lambda}\right) \frac{\lambda_{0J}}{\lambda-\mu^*}$$

$(J\neq 0$, strong coupling)

$$\delta\lambda_{eff} = \frac{(1+\mu^*)^2}{(1+\lambda)^3} \sum_{J\neq 0} \frac{[\lambda_{0J}-\mu^*_{0J}(1+\lambda)/(1+\mu^*)]^2}{(\lambda-\mu^*) - (\lambda-\mu^*)_{JJ}}$$

$$\approx \frac{(1+\mu^*)^2}{(1+\lambda)^3} \sum_{J\neq 0} \frac{\lambda_{0J}^2}{\lambda-\mu^*} \approx \frac{(1+\mu^*)^2}{(1+\lambda)^3(\lambda-\mu^*)} \left[\langle\lambda_k^2\rangle - \lambda^2\right] \tag{36}$$

(strong coupling, weak anisotropy)

The last form of eq. (36) is written in a form which can be calculated in a conventional way without the use of Fermi surface harmonics. The function $\lambda_k$ is the mass enhancement parameter at point k on the Fermi surface

$$\lambda_k = \sum_{k',i} (|M^i_{kk'}|^2/\omega^i_{k-k'})\ \delta(\varepsilon_{k'})$$

$$= \sum_J \lambda_{0J}\ F_J(k) \tag{36a}$$

$$\langle\lambda_k^2\rangle = \frac{1}{\nu}\sum_k \lambda_k^2\ \delta(\varepsilon_k) = \sum_J \lambda_{0J}^2. \tag{36b}$$

This function is one which in certain metals can be extracted from normal state data such as cyclotron resonance, and has been calculated theoretically in non-transition elements by many authors. We make use of the last form of eq. (36) at the end of our paper as an independent check on the accuracy of our expansions.

The effect of anisotropy in $\underset{\sim}{\Lambda}$ is to reduce the gap anisotropy $\Delta_J/\Delta_o$ (for fixed coupling constants $\lambda_{0J}$) by a factor $(1+\lambda)/(1+\mu^*)$, and to reduce $\delta\lambda_{eff}$ by the square of this quantity. The third $(1+\lambda)^{-1}$ term in eq. (36) for $\delta\lambda_{eff}$ is the strong-coupling correction from the isotropic part of the renormalization $\underset{\sim}{\Lambda}$. Remarkably, all the strong coupling corrections cancel in eq. (35) leaving this equation correct provided $\lambda_{eff}$ is written as $(\lambda-\mu^*)/(1+\lambda)$, the coupling constant of an isotropic superconductor. Thus we can rewrite eq. (35),

$$\delta T_c/T_c(iso) = \alpha^2 \ln(\omega_{log}/1.2T_c(iso)). \tag{37}$$

This formula has been derived allowing for strong coupling provided $\lambda \lesssim 1.5$ and arbitrary from of (weak) anisotropy. A few additional comments should be made about these perturbative results. We see that anisotropy always increases $T_c$. This was well known for the weak coupling case ignoring Coulomb repulsion, but is less obvious in the general case. In particular, suppose the electron-phonon interaction is isotropic but the Coulomb interaction is not. Then the gap will be locally depressed at values of k where the Coulomb coupling strength is strong and enhanced where it is weak. This gives rise to a $T_c$ enhancement that is just as strong as if the signs were reversed and it had been the phonon interaction which was anisotropic. If Coulomb and phonon interactions have the same type of anisotropy, cancellations occur which weaken the gap anisotropy and the resulting $T_c$ enhancement. The role of Coulomb and phonon interactions is not completely parallel in this problem (i.e. note the factor $(1+\lambda)/(1+\mu^*)$ which strengthens the role of Coulomb anisotropy in eqs. (36). The reason for the lack of parallelism is that Coulomb effects do not occur in the renormalization matrix $\underset{\sim}{1} + \underset{\sim}{\Lambda}$. It is assumed that Coulomb alterations of the normal metal spectrum are included in the band structure $\epsilon_k$.

The rest of this section gives an outline of the somewhat tedious derivation of eqs. (36). We seek the maximum eigenvalue and the corresponding right eigenvector of the matrix $(1+\Lambda)^{-1}(\lambda-\mu^*)$. Although the matrices involved are all individually symmetric, the product of two symmetric matrices is no longer symmetric, and this gives rise to an important alteration in the algebra. The matrix $\underset{\sim}{\Lambda}$ becomes $\lambda\underset{\sim}{1}$ in the isotropic limit. Thus it is convenient to make some changes in notation

$$\underset{\sim}{1} + \underset{\sim}{\Lambda} \equiv (1 + \lambda)(\underset{\sim}{1} + \underset{\sim}{\chi}) \tag{37}$$

$$(\underset{\sim}{1} + \underset{\sim}{\gamma})^{-1}(\underset{\sim}{\lambda} - \underset{\sim}{\mu}^*) \equiv \underset{\sim}{B} = \underset{\sim}{B}^{(0)} + \underset{\sim}{B}^{(1)} + \underset{\sim}{B}^{(2)} + \ldots \tag{38}$$

We now seek the maximum eigenvalue and corresponding right eigenvector of the matrix $\underset{\sim}{B}$ which differs from $(1+\Lambda)^{-1}(\lambda-\mu^*)$ by the constant factor $(1+\lambda)^{-1}$. Factoring out $(1+\lambda)$ does not affect eigenvectors of $\underset{\sim}{B}$, but we must remember when we are all through to divide the eigenvalue by $(1+\lambda)$. The matrix elements of $\underset{\sim}{\chi}$ and the off-diagonal elements of $\underset{\sim}{\lambda}$ and $\underset{\sim}{\mu}^*$ all vanish in the isotropic limit and are therefore the small parameters of our perturbation theory. The matrix $\underset{\sim}{B}$ is then expanded in powers of these small terms. The leading term, $\underset{\sim}{B}^{(0)}$, is diagonal, and the first and second order terms are denoted $\underset{\sim}{B}^{(1)}$ and $\underset{\sim}{B}^{(2)}$. The formulas of the Rayleigh-Ritz perturbation series are



$$\Delta_J/\Delta_o = B^{(1)}_{JO}/(B^{(0)}_{oo} - B^{(0)}_{JJ}) \qquad (J\neq 0) \tag{39}$$

$$\delta\lambda_{eff} = (1+\lambda)^{-1}\{B^{(1)}_{oo} + B^{(2)}_{oo} + \sum_{J\neq 0} B^{(1)}_{OJ} B^{(1)}_{JO}/(B^{(0)}_{oo} - B^{(0)}_{JJ})\} \tag{40}$$

where it is important to remember that $B_{OJ}$ and $B_{JO}$ are not identical. We can construct the matrix $(1+\gamma)^{-1}$ perturbatively and find the necessary formulas for the elements of $\underset{\sim}{B}$,

$$\underset{\sim}{B} = (\underset{\sim}{1} - \underset{\sim}{\chi} + \underset{\sim}{\chi}^2 - \ldots)(\underset{\sim}{\lambda} - \underset{\sim}{\mu}^*)$$

$$B^{(0)}_{JJ} = (\underset{\sim}{\lambda} - \underset{\sim}{\mu}^*)_{JJ}$$

$$B^{(1)}_{oo} = 0$$

$$B^{(2)}_{oo} = -\sum_{J\neq 0}[\gamma_{OJ}(\underset{\sim}{\lambda}-\underset{\sim}{\mu}^*)_{JO} - \gamma_{OJ}\gamma_{JO}(\underset{\sim}{\lambda}-\underset{\sim}{\mu}^*)_{oo}]$$

$$B^{(1)}_{OJ} = (\underset{\sim}{\lambda} - \underset{\sim}{\mu}^*)_{OJ} - \gamma_{OJ}(\lambda - \mu^*)_{JJ}$$

$$B^{(1)}_{JO} = (\lambda - \mu^*)_{JO} - \gamma_{JO}(\lambda - \mu^*)_{oo} \tag{41}$$

Finally, we need the formula for $\gamma_{JO} = \gamma_{OJ}$,

$$\gamma_{OJ} = (1+\lambda)^{-1}\Lambda_{OJ} = (1+\lambda)^{-1}\sum_{J'} C_{OJJ'}\lambda_{J'o}$$

$$= (1 + \lambda)^{-1}\lambda_{JO} \tag{42}$$

where we have used the definition (8) of $\Lambda_{JJ'}$ and the fact that $C_{OJJ'} = \delta_{JJ'}$. Combining eqs. (39), (41), (42), we easily get the formula (36) for the eigenvector $\Delta_J/\Delta_o$. Deriving the formula (36) for $\delta\lambda_{eff}$ is similarly straightforward but involves a delicate cancellation of the terms in eq. (40).

## IV. THE TWO BAND MODEL

In this section we specialize the results of section II to the case of a two band model[7,8]. This model is exact if the interaction $V_{ph}(k,k')=|M_{kk'}|^2/\hbar\omega_{k-k'}$ has the form

$$V_{ph}(k,k') = \sum_{\alpha,\beta} V_{\alpha\beta}\, \delta_{k\alpha}\, \delta_{k'\beta} \tag{43}$$

where $V_{\alpha\beta}$ are arbitrary positive numbers, $\alpha,\beta$ run over two sheets of Fermi surface (which we label a and b), and the delta's $\delta_{ka}$, $\delta_{kb}$ are 1 if k is on sheet a, b respectively, and zero otherwise. The reason for exhibiting this case explicitly are: first, it is the simplest example of the application of our equations to a situation of some intrinsic interest; and second, we can anticipate in a simple context some of the complexities that will arise when we apply these methods to an actual Fermi surface, that of Nb, which has many different sheets.

Within the two band model, the only band structure information required besides the interaction parameters $V_{\alpha\beta}$ is the partial densities of states $\nu_\alpha$

$$\nu_\alpha = \sum_k \delta_{k\alpha}\, \delta(\varepsilon_k) \tag{44}$$

where the total density of states $\nu$ equals $\nu_a + \nu_b$. As described in ref. 20, one way to construct Fermi surface harmonics is to construct two different sets, $F_{Ja}$ and $F_{Jb}$, each of which vanishes on the opposite sheet. Thus $F_{Ja}$ is automatically orthogonal to $F_{J'b}$ for all J and J'. With the two-band potential (43), it is only necessary to keep the constant function on each sheet, and we denote them $F_a$ and $F_b$. Using the orthonormality relation (3), we get explicit formulas for the normalized FSH's

$$F_a = \sqrt{\nu/\nu_a}\, \delta_{ka} \equiv |a\rangle$$

$$F_b = \sqrt{\nu/\nu_b}\, \delta_{kb}. \equiv |b\rangle \tag{45}$$

The $\underset{\sim}{\lambda}$ matrix has elements defined in eq. (7) which can be written using an inner product notation

$$\lambda_{\alpha\beta} = \nu\langle\alpha|V_{kk'}|\beta\rangle = \sqrt{\nu_\alpha \nu_\beta}\, V_{\alpha\beta} \quad . \tag{46}$$



In the weak-coupling approximation with Coulomb coupling ignored (which is the model solved by Suhl et al[7]), $T_c$ is determined by eq. (27) with $\lambda_{eff}$ the maximum eigenvalue of the 2×2 matrix $\underset{\sim}{\lambda}$. This gives the answer found by Suhl et al[7]. We now examine the strong-coupling corrections.

The functions (45) differ slightly from the choice of FSH's described in section I and implicitly used up to now. The difference is that previously we have assumed that there was a function $F_0=1$, whereas with two distinct sheets it is more natural to use the choice (45). However, it is still possible to revert back to our former convention by making a unitary transformation, and there are certain advantages to doing so. The advantages are that the previous choice correctly simplifies to a 1×1 problem in the isotropic limit, whereas the present choice remains 2×2. (The isotropic limit here is obtained if $V_{\alpha\beta} = V$.) In the case of weak anisotropy it is much easier to do perturbation theory in the former picture. However, the present picture is more natural for doing calculations of the coefficients. These two pictures have been given the names[20] symmetric (S) (for the previous one) and disjoint (D) representation. The transformation equations

$$\begin{pmatrix} F_o \\ F_u \end{pmatrix} = \underset{\sim}{U} \begin{pmatrix} F_a \\ F_b \end{pmatrix}$$

$$\underset{\sim}{U} = \begin{pmatrix} \cos\theta & \sin\theta \\ -\sin\theta & \cos\theta \end{pmatrix}$$

$$\theta = \tan^{-1}\sqrt{\nu_b/\nu_a}, \quad \cos\theta = \sqrt{\nu_a/\nu}, \quad \sin\theta = \sqrt{\nu_b/\nu}$$

$$(\underset{\sim}{\lambda})_{sym} = \underset{\sim}{U}\, (\underset{\sim}{\lambda})_{disj}\, \underset{\sim}{U}^{-1} \tag{47}$$

define a unitary transformation from the disjoint to the symmetric representation. Note that $F_o$ is 1 as required, and $F_u$ orthogonal to $F_o$.

Another advantage of the symmetric representation is that construction of the matrix $\underset{\sim}{\Lambda}$ is conceptually somewhat simpler. A rigorous definition of $\Lambda_{JJ'}$ ( in any orthornormal basis set) is eq. (8) which can be written

$$\Lambda_{JJ'} = \nu^{-1} \sum_{kk'} F_J(k) F_{J'}(k) V_{ph}(k,k') \delta(\varepsilon_k) \delta(\varepsilon_{k'}) \tag{47}$$

where $F_J$ and $F_{J'}$ both have the argument k. Now $V_{ph}$ has by definition the expansion

$$V_{ph}(k,k') = \nu^{-1} \sum_{JJ'} \lambda_{JJ'} F_J(k) F_J(k') \tag{48}$$

We also define coefficients $C_{JJ'J''}$ and $\theta_J$ by

$$\nu^{-1} \sum_k F_J(k) F_{J'}(k) F_{J''}(k) \delta(\varepsilon_k) \equiv C_{JJ'J''} \tag{49}$$

$$\nu^{-1} \sum_k F_J(k) \delta(\varepsilon_k) \equiv \theta_J . \tag{50}$$

Using eqs. (48-50), eq. (47) becomes

$$\Lambda_{JJ'} = \sum_{J''J'''} C_{JJ'J''} \theta_{J'''} \lambda_{J''J'''} . \tag{51}$$

In the symmetric representation, $\theta_J$ equals $\delta_{J0}$ and we recover eq. (8) which is valid in the symmetric representation only. In the disjoint representation, however, the coefficients $\theta$ are less simple, namely $\theta_\alpha = \sqrt{\nu_\alpha/\nu}$ . Thus the more complicated equation (51) must be used. This complication is offset by the simplicity of the resulting formulas for $\Lambda_{\alpha\beta}$. The only non-zero Clebsh-Gordon coefficients are of the type $C_{\alpha\alpha\alpha} = \sqrt{\nu/\nu_\alpha}$ which implies that $\Lambda$ is diagonal in the disjoint representation of the 2-band model,

$$(\Lambda_{\alpha\beta})_{disj} = \delta_{\alpha\beta} \sum_\gamma \sqrt{\frac{\nu_\gamma}{\nu_\alpha}} \lambda_{\alpha\gamma} \tag{52}$$

$$(\underset{\sim}{\Lambda})_{sym} = \underset{\sim}{U} (\underset{\sim}{\Lambda}_{disj}) \underset{\sim}{U}^{-1} . \tag{53}$$

We can now solve for $T_c$ in either representation. The disjoint representation proves simpler because $\underset{\sim}{\Lambda}$ is diagonal. We can factor $(\underset{\sim}{1} + \underset{\sim}{\Lambda})$ into $[(\underset{\sim}{1} + \underset{\sim}{\Lambda})^{\frac{1}{2}}]^2$ and then seek the maximum eigenvalue of



$$\underset{\sim}{\lambda}^* \equiv (\underset{\sim}{1}+\underset{\sim}{\Lambda})^{-\frac{1}{2}} (\underset{\sim}{\lambda}-\underset{\sim}{\mu}^*) (\underset{\sim}{1}+\underset{\sim}{\Lambda})^{-\frac{1}{2}}$$

$$(\lambda^*_{\alpha\beta})_{disj} = (\lambda_{\alpha\beta} - \mu^*_{\alpha\beta}) / \sqrt{(1+\Lambda_{\alpha\alpha})(1+\Lambda_{\beta\beta})} . \tag{54}$$

The final formula for $\lambda_{eff}$ is

$$\lambda_{eff} = \tfrac{1}{2}(\lambda^*_{aa} + \lambda^*_{bb}) + \sqrt{[\tfrac{1}{2}(\lambda^*_{aa} - \lambda^*_{bb})]^2 + \lambda^*_{ab}{}^2} \tag{55}$$

We believe that this is the first time the complete solution of the strongly coupled two-band model has been given. A correct result was given by Geilikman and Masharov[27], except they have folded the renormalization $\Lambda$ into the coupling constant $\lambda$, and have not provided the connection (52) between the mass renormalization and the coupling constant matrix.

## V. CONSTRUCTING FERMI SURFACE HARMONICS

There are two parts to the problem of constructing FSH's: first, enumerating a maximal set of linearly independent polynomials of a given symmetry type, and second, orthogonalizing them. Both of these involve standard mathematical procedures, but it seems appropriate to give a summary of the procedures we have found useful.

First we work out the case where there is a single sheet of Fermi surface. It does not matter whether this sheet is open as in the Fermi surface of Cu or the "jungle-gym" of Nb, or closed as the "jack" of Nb; the form of the functions is the same. The task is to construct orthonormal polynomials starting with zeroth order and increasing in order until convergence is obtained for the problem at hand. In $N^{th}$ order there are in general $(N+1)(N+2)/2$ linearly independent functions of the form $v_x^\ell v_y^m v_z^n$ with $\ell,m,n > 0$ and $\ell + m + n = N$. The operation R of the point group G of the crystal transforms points in k space into new points $R^{-1}k$. When the operations R are performed on the polynomials, they will transform into other polynomials of the same order. A trivial example is the zero order polynomial, 1, which is invariant under all operations R, and thus transforms according to the identity representation $\Gamma_1$, of G. The first order polynomials are the three components of the velocity. The velocity vector $v_k$ transforms into $v_{R^{-1}k} = \Gamma(R) v_k$, and the matrices $\Gamma(R)$ form a representation of the group G. For cubic symmetry this is the irreducible representation $\Gamma_{15}$ (in the notation of Bouchaert, Smoluchowski, and Wigner[28]). For lower symmetry the representation $\Gamma$ thus defined is a reducible representation.

From now on we will assume the crystal has cubic symmetry. The four functions (1, $v_x$, $v_y$, $v_z$) so far discussed are automatically orthogonal because they belong either to different representations or to different rows of the same irreducible representation. Normalizing the functions is easy: 1 is already normalized by the definitions (3), and is given the name $F_o$. The remaining three are normalized by dividing by $\langle v_x^2\rangle^{\frac{1}{2}} = (\frac{1}{3}\langle v^2\rangle)^{\frac{1}{2}}$ where $\langle v^2\rangle^{\frac{1}{2}}$ is the rms Fermi velocity. These functions are named $F_x$, $F_y$, $F_z$. In second order there are six polynomials, $v_x^2$, $v_y^2$, $v_z^2$, $v_xv_y$, $v_yv_z$, $v_zv_x$. These form a reducible six-dimensional representation of G. It is clear that in cubic symmetry the first three do not mix with the other three, so the representation can be immediately reduced to two three-dimensional representations. The general process of reduction is illustrated in Table I, where the character table of the cubic group is given. Only even representations and proper rotations are displayed explicitly. It is all that is necessary because in the examples worked below, it is always obvious whether the representations are even or odd. The characters (traces) of the 6×6 matrices for the second order polynomials are easily worked out and are displayed in the row labled $\Gamma_{vv}$ in Table I. Using the orthogonality relation for characters, it is found that $\Gamma_{vv}$ reduces to $\Gamma_1 + \Gamma_{12} + \Gamma_{25'}$. Thus the three functions $v_xv_y$, $v_yv_z$, $v_zv_x$ are basis functions for the irrdeucible representation $\Gamma_{25'}$, while the functions $v_x^2$, $v_y^2$, $v_z^2$ can be further reduced to $\Gamma_1 + \Gamma_{12}$. It is also clear that $v^2 = v_x^2 + v_y^2 + v_z^2$ is a totally symmetric ($\Gamma_1$) function, and $\Gamma_{12}$ functions can easily be found ($v_x^2 - v_y^2$ and $3v_z^2 - v^2$ are conventional choices, but there is no rule that specifies *a priori* which linear combinations or signs should be chosen. Once a choice has been made, however, the higher order $\Gamma_{12}$ functions are constrained except for signs.). Of the six new functions, five are automatically orthogonal to the lower ones but $v^2$ is not orthogonal to $F_o$. Our specific conventions and proceduces for doing the orthogonalization will be discussed below.

The reduction of higher order functions proceeds in a similar fashion. The results of the character analysis for N=3, 4 and 6 are in Table I. The explicit construction of linearly independent functions with the proper transformation properties can usually be accomplished by intuition assisted by simple rules, but projection operator techniques are also available if intuition fails. Usually only the $\Gamma_1$ and $\Gamma_{15}$ representations will be of interest (for use in superconductivity and transport, respectively). There are two $\Gamma_{15}$ sets in third order. One is trivial - the product of the first order $\Gamma_{15}$ functions and the second order $\Gamma_1$ function, namely $v^2v_x$, $v^2v_y$, $v^2v_z$. The other is a new set, $v_x^3$, $v_y^3$, $v_z^3$. Similarly the fourth order $\Gamma_1$ functions are trivial ones; $(v^2)^2$, and a new one, $v_x^4 + v_y^4 + v_z^4$. If we stop at fourth order, we have a total of four $\Gamma_1$ functions which we can put into orthonormal form, and group theory assures us that there are no more to be found without going to higher order.



TABLE I

Character table of cubic group, and characters of $n^{th}$ order polynomials for $n \leq 4$ on a single sheet and on a set of 6 equivalent sheets centered at the N point of the bcc Brillouin zone.

| label of representation \ class | E | $3C_4^2$ | $6C_4$ | $6C_2$ | $8C_3$ | decomposition of reducible representation |
|---|---|---|---|---|---|---|
| $\Gamma_1$ | 1 | 1 | 1 | 1 | 1 | |
| $\Gamma_2$ | 1 | 1 | -1 | -1 | 1 | |
| $\Gamma_{12}$ | 2 | 2 | 0 | 0 | -1 | |
| $\Gamma_{15'}$ | 3 | -1 | 1 | -1 | 0 | |
| $\Gamma_{25'}$ | 3 | -1 | -1 | 1 | 0 | |
| $\Gamma_c$ | 1 | 1 | 1 | 1 | 1 | $\Gamma_1$ |
| $\Gamma_\chi$ | 3 | -1 | 1 | -1 | 0 | $\Gamma_{15}$ |
| single sheet $\Gamma_{\chi\chi}$ | 6 | 2 | 0 | 2 | 0 | $\Gamma_1 + \Gamma_{12} + \Gamma_{25'}$ |
| single sheet $\Gamma_{\chi\chi\chi}$ | 10 | -2 | 0 | -2 | 1 | $\Gamma_{2'} + 2\Gamma_{15} + \Gamma_{25}$ |
| $\Gamma_{\chi\chi\chi\chi}$ | 15 | 3 | 1 | 3 | 0 | $2\Gamma_1 + 2\Gamma_{12} + \Gamma_{15'} + 2\Gamma_{25'}$ |
| $\Gamma_v^6$ | 28 | 4 | 0 | 4 | 1 | $3\Gamma_1 + \Gamma_2 + 3\Gamma_{12} + 2\Gamma_{15'} + 4\Gamma_{25'}$ |
| $\Gamma_c$ | 6 | 2 | 0 | 2 | 0 | $\Gamma_1 + \Gamma_{12} + \Gamma_{25'}$ |
| $\Gamma_\chi$ | 18 | -2 | 0 | -2 | 0 | $\Gamma_{2'} + \Gamma_{12'} + 3\Gamma_{15} + 2\Gamma_{25}$ |
| N point ellipsoids $\Gamma_{\chi\chi}$ | 36 | 4 | 0 | 4 | 0 | $3\Gamma_1 + \Gamma_2 + 4\Gamma_{12} + 3\Gamma_{15'} + 5\Gamma_{25'}$ |
| N point ellipsoids $\Gamma_{\chi\chi\chi}$ | 60 | -4 | 0 | 0 | 0 | $2\Gamma_{1'} + 2\Gamma_{2'} + 4\Gamma_{12'} + 8\Gamma_{15} + 8\Gamma_{25}$ |
| N point ellipsoids $\Gamma_{\chi\chi\chi\chi}$ | 90 | 6 | 0 | 10 | 0 | $7\Gamma_1 + 2\Gamma_2 + 9\Gamma_{12} + 8\Gamma_{15'} + 13\Gamma_{25'}$ |

The next $\Gamma_1$ functions are sixth order. The intuitive method suggests four basis functions, two "old ones", $v_2^6$ and $v^2(v_x^4 + v_y^4 + v_z^4)$, and two "new ones", $v_x^6 + v_y^6 + v_z^6$ and $v_x^2 v_y^2 v_z^2$. However, group theory shows that only three $\Gamma_1$ functions occur in sixth order. The four we have listed are actually linearly dependent, because $v^6 = 3v^2(v_x^4 + v_y^4 + v_z^4) + 6v_x^2 v_y^2 v_z^2 - 2(v_x^6 + v_y^6 + v_z^6)$. We can choose any three of these four functions as the maximal linearly independent set.

The second example is a case where the Fermi surface has multiple sheets which are related to each other by the symmetry operations of the crystal. Specifically, Nb has surfaces at the N or $(\pi/a)(110)$ points. There are twelve half-surfaces or 6 whole surfaces in the first Brillouin zone, and we refer to them as "potatoes" because of their distorted ellipsoidal shape. Each potato individually has orthorhombic symmetry, but the collection of six potatoes has full cubic symmetry. Here we pretend no other sheets occur besides the six potatoes. In actual application to Nb, the normalizations will need to be altered because two additional sheets occur.

We now have six times as many linearly independent functions in each order as we had before. For example in zeroth order we can choose $F_a$ to be $\sqrt{v/v_a}$ on potato "a" in the [110] direction and zero elsewhere. Similarly there are functions $F_b$, $F_c$, $F_d$, $F_e$, $F_f$, corresponding to potatoes "b" in the $[1\bar{1}0]$ direction, "c" in the [011] direction, "d" in the $[01\bar{1}]$ direction, "e" in the [101], and "f" in the $[\bar{1}01]$ direction. These six functions are clearly linearly independent and orthonormal in the sense of eq. (3). Under the operations R these functions transform into each other, forming a six-dimensional reducible representation. From Table I we see that this reduces to $\Gamma_1 + \Gamma_{12} + \Gamma_{25}'$. The $\Gamma_1$ function will clearly be $F_o = 1 = \sqrt{v_a/v}\,(F_a+F_b+F_c+F_d+F_e+F_f)$ which is totally symmetric. The function $F_a-F_b$ is clearly orthogonal to $F_o$ and along with its partners $F_c-F_d$, $F_e-F_f$, form the basis of the $\Gamma_{25}'$ representation. Finally, $F_c+F_d-F_e-F_f$ and $3(F_a+F_b)-F_o$ from the two $\Gamma_{12}$ partners.

In doing character analysis for multipy-sheeted Fermi surfaces, it is not necessarily true that even polynomials will belong to even representations. For example, if two sheet transform into each other under inversion, then the constant polynomial which is 1 on the first sheet, -1 on the second, is odd. This is not possible on the Nb potatoes because each sheet transforms into itself under inversion, and even or odd polynomials always belong to even or odd representations respectively.

We need explicit formulas for the 3 linearly independent second order $\Gamma_1$ polynomials on the potatoes. These are most simply found by examining the subgroup that leaves a single potato invariant. There are three orthogonal axes with $C_2$ operations, in the [110], [110] and [001] directions respectively for the "a" potato. Correspondingly the polynomials $(v_x + v_y)^2$, $(v_x - v_y)^2$, and $v_z^2$ are invariants under this subgroup. Each of these generates a $\Gamma_1$ function of the full group if we operate on it by the six operations which generates the six potatoes and add the results in phase. Thus for example, $v_z^2$ generates a functions $v_z^2(\delta_{ka}+\delta_{kb}) + v_x^2(\delta_{kc}+\delta_{kd}) + v_y^2(\delta_{ke}+\delta_{kf})$ which has $\Gamma_1$ symmetry. We have chosen $v^2$, $v_z^2$ and $v_x v_y$ as a convenient choice of three independent $\Gamma_1$ functions on potato "a" which generate $\Gamma_1$ functions on the full serface.



This concludes the outline of how the maximal set of linealy independent functions is found. We now outline the procedures we followed in orthornormalizing them. We consider only the $\Gamma_1$ subset, and list the linearly independent functions in order starting with polynomials of lowest degree. The ordering of functions of the same degree can be chosen arbitrarily and must be clearly specified because it affects the form of the function. We label the linearly independent set $f_1$, $f_2$.... Our task is to construct an orthonormal set $F_1$, $F_2$.... This is done by the usual Gram-Schmidt procedure

$$F_1 = f_1/\text{norm}_1$$

$$F_2 = [f_2 - \langle F_1 | f_2 \rangle F_1]/\text{norm}_2$$

$$F_n = [f_n - \sum_{j=1}^{n-1} \langle F_J | f_n \rangle F_j]/\text{norm}_n. \tag{56}$$

We find it convenient to keep track of the transformation matrix T, from the $f_j$'s to the $F_i$'s.

$$F_i = \sum_{j \le i} T_{ij} f_j \tag{57}$$

$$A_{ij} \equiv \langle f_i | f_j \rangle. \tag{58}$$

The matrix T has positive diagonal elements and zeros on every location above the diagonal. It is relatively easy to express $T_{ij}$ in terms of the matrix $A_{ij}$ of the overlaps of the original functions. Finally, we need to know expansion coefficients $p_J$ and $Q_{JJ'}$ of functions p(k) and operators Q(k,k') in the FSH basis. We find it more convenient to calculate first in the non-orthogonal basis of $f_i$'s and then transform

$$p_J = \sum_i T_{ji} \langle f_i|p\rangle$$

$$Q_{JJ'} = \sum_{ii'} T_{ji} \langle f_i|Q|f_{i'}\rangle (T^{tr})_{i'J'}. \quad (59)$$

There are two reasons for doing all the calculations first in the nonorthogonal basis and then transforming. One is that often integrals like $\langle f_i|p\rangle$ are interesting in their own right, or more easily interpreted than the more abstract $\langle F_J|p\rangle$. The other reason is that this enables us to do all the Fermi surface integrals simultaneously. That is, our computer programs do Fermi surface integrals such as $\langle f_i|f_j\rangle$ which are needed to construct orthonormal functions, and at the same time integrals such as $\langle f_i|p\rangle$ are done which are later used to find $p_J$. After all the integrals are done, a separate program is written which constructs the matrix $\underset{\sim}{T}$ from the coefficients $A_{ij}$ and then constructs $p_J$ and $Q_{JJ'}$.

Finally, since Nb has three separate types of Fermi surface, it is necessary to decide which representation to work in, disjoint (D) or symmetric (S). There are several reasons for preferring the D-representation in the numerical calculations. The most compelling one is that our programs do integrals over the three types of surface by somewhat different procedures and at different places in the program. This makes it difficult to do integrations over functions which are non-zero on more than one type of surface. When the calculations are all done, it is desirable to transform to the S-representation so that perturbation theory for weak anisotropy can be used. For this purpose, only the constant functions need to be in the S-representation - the functions derived from higher order polynomials can be left untouched. Thus the matrix U which transforms D → S is the unit matrix except for a 3×3 sub-block which describes how the three constant functions transform. This sub-block was chosen in the form

$$U = \begin{pmatrix} \cos\theta & \sin\theta\cos\phi & \sin\theta\sin\phi \\ 0 & \sin\phi & -\cos\phi \\ \sin\theta & -\cos\theta\cos\phi & -\cos\theta\sin\phi \end{pmatrix}$$

$$\cos\theta = \sqrt{\nu_a/\nu},\ \sin\theta\cos\phi = \sqrt{\nu_b/\nu},\ \sin\theta\sin\phi = \sqrt{\nu_c/\nu}$$

$$F_J(S) = \sum_{J'} U_{JJ'} F_{J'}(D) \quad (60)$$

where $\nu_\alpha$ is the partial density of states of the band $\alpha$. The functions $F_J(D)$ are the form $\sqrt{\nu/\nu_\alpha}\,\delta_{k\alpha}$, ($\alpha$ = a,b,c). Applying the transformation



(60), the first of the S functions has the form $\sum_\alpha \delta_{k\alpha} = 1$, and is the function we have previously labeled $F_o$.

We have made no effort to calculate the $\underset{\sim}{\mu}^*$ matrix from first principles. Therefore we make the simplest possible assumptions, namely that $\underset{\sim}{\mu}^*$is isotropic. This means that in the S-representation we get $\mu^*_{JJ'}(S) = \mu^* \delta_{J0}\delta_{J'0}$. The matrix $\underset{\sim}{\mu}^*$in the D-representation can be found using the inverse of the transformation (60) (equal to the transpose of the unitary matrix $\underset{\sim}{U}$), namely $\underset{\sim}{\mu}^*(D) = \underset{\sim}{U}^{-1}\,\underset{\sim}{\mu}^*(S)\,\underset{\sim}{U}$.

## VI. CALCULATION OF THE MATRIX $\lambda_{JJ'}$ FROM FIRST PRINCIPLES BAND THEORY

In this section we show that if one neglects anisotropy arising from the phonons, the matrix $\lambda_{JJ'}$ can be obtained rather simply from a sufficiently detailed energy band calculation. Let us define a new matrix, $\eta_{JJ'}$, by

$$\eta_{JJ'} = 2M \int_0^\infty d\Omega\ \Omega\ \alpha^2_{JJ'} F(\Omega)$$

$$= \frac{M}{\nu} \sum_{kk',i} |M^i_{kk'}|^2\ \omega^i_{k-k'} F_J(k)\ F_{J'}(k')\ \delta(\varepsilon_k)\ \delta(\varepsilon_{k'}) . \quad (61)$$

$\eta_{JJ'}$ is a generalization of the quantity $\eta$ introduced by McMillan[5] and Hopfield[29], related to $\lambda_{JJ'}$ through the identity

$$\lambda_{JJ'} = \eta_{JJ'}/M\ \Omega^2_{JJ'}\ , \quad (62)$$

where the average square frequency, $\langle\Omega^2\rangle_{JJ'}$, is given by

$$\langle\Omega^2\rangle_{JJ'} = \int_0^\infty d\Omega\ \Omega\ \alpha^2_{JJ'} F(\Omega) \Big/ \int_0^\infty d\Omega/\Omega\ \alpha^2_{JJ'} F(\Omega) \quad (63)$$

For $J = J' = 0$ it is usually a good approximation to replace $\langle\Omega^2\rangle_{JJ'}$ by $\langle\Omega^2\rangle$ where $\langle\Omega^2\rangle$ is obtained by neglecting the frequency dependence of $\alpha^2_{JJ'}$ in Eq. (63). We shall assume $\langle\Omega^2\rangle_{JJ'} = \langle\Omega^2\rangle$ in the following for all J and J'. This has the effect of omitting the phonon contribution to the gap anisotropy.

The computational advantage of working with $\eta_{JJ'}$ as opposed to $\lambda_{JJ'}$ is that $\eta_{JJ'}$ may be written in terms of single (rather than

double) integrals over the Fermi surface. In addition $\eta_{JJ'}$ depends only upon the electronic structure of the system. The phonons enter $\lambda_{JJ'}$ in this approximation only through the denominator $M\,\Omega^2$. These simplifications result from the fact that the factor $M\omega^i_{k-k'}$ in Eq. (61) cancels against a similar factor coming from the matrix elements,

$$M^i_{kk'} = \int d^3r\ \psi^*_k(r)\ \hat{\epsilon}^i_{k-k'} \cdot \nabla V\ \psi_{k'}(r)/\sqrt{M\omega^i_{k-k'}}\ . \tag{64}$$

The matrix element contains electronic wave function $\psi_k(r)$, a phonon polarization vector $\hat{\epsilon}^i_{k-k'}$, a potential gradient $\nabla V$, the ionic mass, M, and phonon frequency $\omega^i_{k-k'}$. It is difficult to calculate $\nabla V$ accurately for a transition metal. We shall use the rigid muffin-tin approximation of Gaspari and Gyorffy[30-32] which seems to give reasonable agreement with empirical values of $\eta$.

Substituting the matrix elements (63) into our expression (61) for $\eta_{JJ'}$ we obtain (using the completeness of the polarization vectors)

$$\eta_{JJ'} = \frac{1}{\nu} \sum_{kk'} \int d^3r \int d^3r'\ \psi^*_k(r)\ \psi_{k'}(r)\ \psi_k(r')\ \psi^*_{k'}(r')\ \nabla V(r) \cdot \nabla' V(r') \times F_J(k)\ F_{J'}(k')\ \delta(\varepsilon_k)\ \delta(\varepsilon_{k'})\ . \tag{65}$$

One easily recognizes in (64) the Fermi-surface density matrix,

$$\rho_k(r,r') = \psi^*_k(r)\ \psi_k(r')\ \delta(\varepsilon_k), \tag{66}$$

and its expansion coefficient in FSH's,

$$\rho_J(r,r') = \frac{1}{\nu} \sum_k \rho_k(r,r')\ F_J(k)\ . \tag{67}$$

Thus, in terms of $\rho_J(r,r')$ we have

$$\eta_{JJ'} = \nu \int d^3r \int d^3r'\ \rho_J(r,r')\ \rho_{J'}(r',r)\ \nabla V(r) \cdot \nabla' V(r')\ . \tag{68}$$

The quantities $\rho_J(r,r')$ must be expanded in coordinate space cubic harmonics in order to make contact with quantities available from band theory.



$$\begin{aligned}\rho_J(r,r') &= \frac{1}{\nu} \sum_k \psi^*_k(r)\ \psi_k(r')\ F_J(k)\ \delta(\varepsilon_k) \\ &= \frac{1}{\nu} \sum_k \sum_{\ell\mu t} \sum_{\ell'\mu' t'} i^{\ell'-\ell}\ c^t_{\ell\mu}(k)\ c^{t'}_{\ell'\mu'}(k)\ R_\ell(r)\ R_{\ell'}(r) \\ &\quad \times K^t_{\ell\mu}(\hat{r})\ K^{t'}_{\ell'\mu'}(\hat{r}')\ \delta(\varepsilon_k) F_J(k)\end{aligned} \tag{69}$$

where we have used the Bloch wave expansion

$$\psi_k(r) = \sum_{\ell\mu t} i^\ell\ c^t_{\ell\mu}(k)\ R_\ell(r)\ K^t_{\ell\mu}(\hat{r})\ . \tag{70}$$

$R_\ell(r)$ is a regular solution to the radial Schrödinger equation, $K^t_{\ell\mu}$ is a cubic harmonic of row $\mu$ of irreducible representation t and orbital quantum number $\ell$, and $c^t_{\ell\mu}$ is an expansion coefficient which is obtained from an energy band calculation. It may be noted that all quantities which enter (68) and (69) are available if a detailed Fermi surface calculation has been performed.

Additional simplifications can be achieved by exploiting the cubic symmetry of Nb. Equation (69) contains the Fermi surface integral

$$T^{tt'}_{\ell\mu,\ell'\mu',J} = \frac{1}{\nu} \sum_k c^t_{\ell\mu}(k)\ c^{t'}_{\ell'\mu'}(k)\ F_J(k)\ \delta(\varepsilon_k)\ . \tag{71}$$

For s-wave superconductitity we are only interested in the $\Gamma_1$ submatrix of $\eta_{JJ'}$. For this reason only FSH's with full cubic symmetry will be considered in Eq. (71), and for this case one can show that $T^{tt'}_{\ell\mu,\ell'\mu'J}$ is diagonal in t and t' and also in $\mu$ and $\mu'$, and independent of $\mu$.

$$T^{tt'}_{\ell\mu,\ell\mu'J} = T^t_{\ell\ell',J}\ \delta_{tt'}\ \delta_{\mu\mu'}\ . \tag{72}$$

Substituting (72) and (71) into (69) we have

$$\rho_J(r,r') = \sum_{\ell\ell',t} T^t_{\ell\ell',J}\ R_\ell(r)\ R_{\ell'}(r')\ F^t_{\ell\ell'}(\hat{r},\hat{r}') \tag{73}$$

where

$$F^t_{\ell\ell'}(\hat{r},\hat{r}') = \sum_\mu K^t_{\ell\mu}(\hat{r})\ K^t_{\ell'\mu}(\hat{r}')\ . \tag{74}$$

The functions $F^t_{\ell\ell'}$ are listed in ref. 32.

At this point it is helpful to condense the notation slightly. One can show that for most values of $(\ell,\ell',t)$, $T^t_{\ell\ell'J}$ is zero. In fact for $\ell,\ell' \leq 3$ there are only 8 non-vanishing coefficients for a given value of J. Thus we write $\alpha$ for the set of indices $(\ell,\ell',t)$, i.e.

$$T^t_{\ell\ell'J} \equiv T^\alpha_J \qquad (\alpha = 1 \ldots 8) \quad . \tag{75}$$

The translation $\alpha \leftrightarrow (\ell\ell' t)$ can be found in Table II.

Using this notation (73) becomes

$$\rho_J(r,r') = \sum_\alpha T^\alpha_J \, R_\ell(r) \, R_{\ell'}(r') \, F_\alpha(\hat{r},\hat{r}') \tag{76}$$

and (68) becomes

$$\eta_{JJ'} = \nu \sum_{\alpha\beta} T^\alpha_J \, T^\beta_{J'} \, g_{\alpha\beta} \tag{77}$$

where the coupling matrix is given by

$$g_{\alpha\beta} = V'_{\ell_1\ell_4} \, V'_{\ell_2\ell_3} \int d\hat{r} \int d\hat{r}' \, F^t_{\ell_1\ell_2}(\hat{r},\hat{r}') \, F^{t'}_{\ell_3\ell_4}(\hat{r}',\hat{r}) \, \frac{(xx' + yy' + zz')}{rr'} \qquad \alpha = (\ell_1\ell_2 t) \qquad \beta = (\ell_3\ell_4 t') \quad . \tag{78}$$

$V'_{\ell_1\ell_4}$ is a radial integral over the derivative of the band theory potential in the rigid muffin-tin approximation.

$$V'_{\ell_1\ell_4} = \int r^2 \, R_{\ell_1}(r) \, R_{\ell_4}(r) \, \frac{\partial V}{\partial r} \, dr \tag{79}$$

$g_{\alpha\beta}$ is displayed explicitly in Table II.

To summarize: $\eta_{JJ'}$ is obtained from (77) where $g_{\alpha\beta}$ is obtained from Table II, and $T^\alpha_J = T^t_{\ell\ell',J}$ is obtained from (71) which we may write as



TABLE II

Coupling constant matrix, $g_{\alpha\beta}$ for Nb. Radial wave functions are normalized to 1 at the muffin-tin radius. The constants are dimensionless.

| $\ell\ell' t$ | $\alpha$ / $\beta$ | $00\Gamma_1$ | $11\Gamma_{15}$ | $22\Gamma_{25'}$ | $33\Gamma_{12}$ | $33\Gamma_{25'}$ | $33\Gamma_{15}$ | $33\Gamma_{2'}$ | $13\Gamma_{15}$ |
|---|---|---|---|---|---|---|---|---|---|
| | | 1 | 2 | 3 | 4 | 5 | 6 | 7 | 8 |
| $00\Gamma_1$ | 1 | 0 | A | 0 | 0 | 0 | 0 | 0 | 0 |
| $11\Gamma_{15}$ | 2 | A | 0 | 6/5 B | 4/5 B | 0 | 0 | 0 | 0 |
| $22\Gamma_{25'}$ | 3 | 0 | 6/5 B | 0 | 0 | 6/7 C | 18/35 C | 3/7 C | $\frac{12}{5}\sqrt{3/7}$ D |
| $22\Gamma_{12}$ | 4 | 0 | 4/5 B | 0 | 0 | 3/7 C | 27/35 C | 0 | $\frac{12}{5}\sqrt{3/7}$ D |
| $33\Gamma_{12}$ | 5 | 0 | 0 | 6/7 C | 3/7 C | 0 | 0 | 0 | 0 |
| $33\Gamma_{15}$ | 6 | 0 | 0 | 18/35 C | 27/35 C | 0 | 0 | 0 | 0 |
| $33\Gamma_{2'}$ | 7 | 0 | 0 | 3/7 C | 0 | 0 | 0 | 0 | 0 |
| $13\Gamma_{15}$ | 8 | 0 | 0 | $\frac{12}{5}\sqrt{3/7}$ D | $-\frac{12}{5}\sqrt{3/7}$ D | 0 | 0 | 0 | 0 |

$A = V'^2_{01} = 11.999$

$B = V'^2_{12} = 19.787$

$C = V'^2_{23} = 306.290$

$D = V'_{12} \, V'_{23} = -77.850$

$$T^t_{\ell\ell',J} = \frac{1}{\nu} \sum_k c^t_{\ell\mu}(k)\ c^t_{\ell'\mu}(k)\ F_J(k)\ \delta(\varepsilon_k) \quad . \tag{80}$$

These Fermi surface integrals are the heart of the numerical calculation. They can be restricted to the irreducible 1/48th of the Brillouin zone by virture of the fact that the quantity,

$$T^t_{\ell\ell'}(k) \equiv \frac{1}{g} \sum_\mu c^t_{\ell\mu}(k)\ c^t_{\ell'\mu}(k) \quad , \tag{81}$$

(where g is the dimensionality of t) has full cubic symmetry. Thus the main numerical effort involves calculation of integrals of the form

$$T^t_{\ell\ell',J} = 48\ \frac{1}{\nu} \sum_{k\varepsilon(1/48)} T^t_{\ell\ell'}(k)\ F_J(k)\ \delta(\varepsilon_k) \quad . \tag{82}$$

The Fermi surface of Nb is shown in the computer generated perspective drawings Figs. 1-3. For each mesh point we have calculated the magnitude of k, the group velocity $\nabla_k\varepsilon$, and the wave functions $c^t_{\ell\mu}(k)$. The details of the calculation are described in ref. 32. All of the points shown were generated from first principles without the use of interpolation schemes, using the KKR constant-energy-search[33] method. This calculation agrees well with the earlier APW calculation by Mattheiss[34].

## VII. COMPLETENESS

The question of whether or not the FSH's for an arbitrary Fermi surface are complete in the mathematical sense was addressed in ref. 20, but the question was not laid to rest. In this section we are concerned with the more practical (and perhaps more important) question of whether or not the functions $T^\alpha(k)$ defined in Eq. (81) can be expanded as a rapidly convergent series of FSH's for Nb. In order to answer this question quantitatively we define a quantity $p^\alpha_{n,s}$ which is the percentage of completeness of the expansion of $T^\alpha(k)$, through nth order FSH's in the disjoint representation on surface s. Thus

$$(p^\alpha_{n,s})^2 = \sum_{J=0}^{n} (T^\alpha_{J,s})^2 / \langle (T^\alpha(k))^2 \rangle_s \tag{83}$$

where

$$\langle (T^\alpha(k))^2 \rangle_s = \frac{1}{\nu} \sum_{k \text{ on } s} \delta(\varepsilon_k)\ (T^\alpha(k))^2 \quad . \tag{84}$$



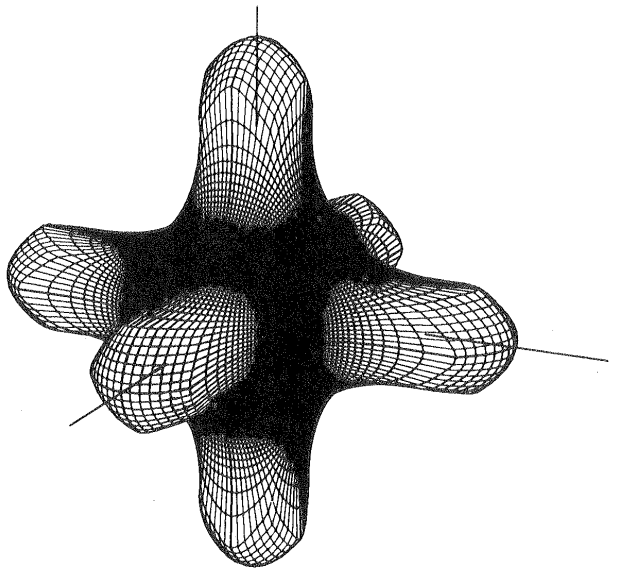

Figure 1: The central sheet or "jack" of Nb containing holes from the second band. Points of discontinuous slope can be seen corresponding to points where this surface touches the surface of fig. 2

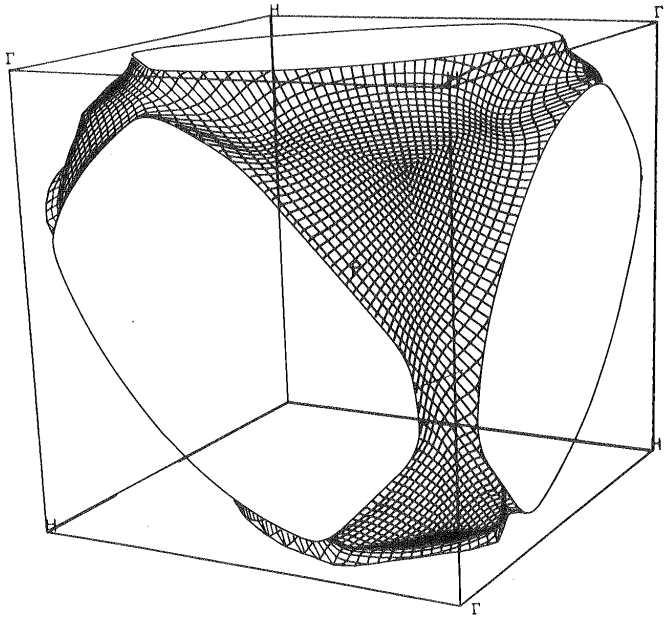


Figure 2: The third band open surface of Nb. In the earlier work by Mattheiss this sheet was drawn centered about Γ, and appears as a jungle-gym containing hole states. From the present perspective centered around P the surface contains electrons and is more reminiscent of a bikini.



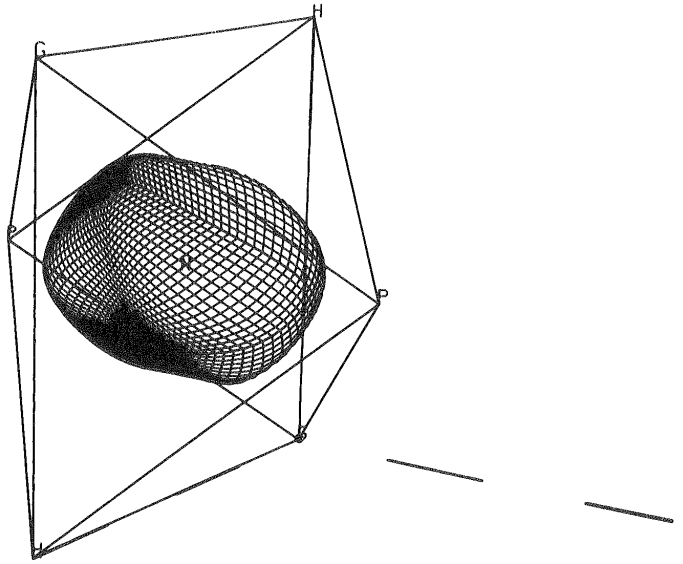


Figure 3: The third band hole surface of Nb centered at the N point. This is one of six such surfaces, called "potatoes", each of which has rhombohedral symmetry.

and where $T^{\alpha}_{J,s}$ is the expansion coefficient of $T^{\alpha}(k)$ on sheet s. If the FSH's were known to be complete, this would guarantee (by the definition of completeness) that the sequence $p_0^2$, $p_1^2$,..$p_n^2$ converge to 1. Since the FSH's are not known to be complete, the empirical convergence of these sequences constitutes an important test of completeness.

We have carried out calculations for Nb using the seven lowest order FSH's on sheets 1 (the jack(fig. 1)) and 2 ( the jungle-gym (fig. 2)), and the four lowest order functions (sheet 3) on the potatoes, (fig. 3). Our specific choices for the unnormalized functions $f_{Js}$ are listed in Table III. The rules given in sec. V provide an unambiguous specification of the resulting FSH's $F_{Js}(k)$. In table IV we present our calculated values of the expansion coefficients $T_{Js}^{\alpha}$ for Nb, and our final value $p_{ns}^{\alpha}$ for the percentage of completeness, where only the final term $n = n_{max}$ is shown explicitly. Typically, about 95% completeness has been achieved. We also give the partial densities of states $\nu_s^{\alpha}$ which are the contributions to the Fermi energy density of states arising from states of type $\alpha$ on sheet s, and $I_{\alpha}$, the integral of the radial wave functions $R_{\ell}(r)$ and $R_{\ell'}(r)$ with appropriate weighting functions over the Wigner Seitz cell.

$$I_{\alpha} = \int d^3r \; R_{\ell}(r) \; R_{\ell'}(r) \; F_{\alpha}(\hat{r},\hat{r}) \quad . \tag{85}$$

The condition that the wave functions be normalized to unity over the Wigner-Seitz cell for each k point leads to the requirement that

$$\sum_{\alpha} T^{\alpha}(k) \; I_{\alpha} = 1 \quad . \tag{86}$$

The integral over a sheet of Eq. (86) leads to

$$\sum_{\alpha} \sum_{k \text{ on } s} T^{\alpha}(k) \; \delta(\varepsilon_k) \; I_{\alpha} = \nu_s \quad . \tag{87}$$

Inclusion of a FSH in the k integral of (87) leads to the following sum rules,

$$\sum_{\alpha} T^{\alpha}_{J,s} \; I_{\alpha} = \sqrt{\nu_s/\nu} \; \delta_{J0} \; . \tag{88}$$



TABLE III

Fermi Surface Harmonics with full cubic symmetry for Nb (non-orthogoanl basis).

| J | sheets 1 & 2 | sheet 3* (potatoes) |
|---|---|---|
| 0 | 1 | $\delta_{ka} + \delta_{kb} + \delta_{kc} + \delta_{kd} + \delta_{ke} + \delta_{kf}$ |
| 1 | $v^2$ | $v^2(\delta_{ka} + \delta_{kb} + \delta_{kc} + \delta_{kd} + \delta_{ke} + \delta_{kf})$ |
| 2 | $v^4$ | $v_z^2(\delta_{ka} + \delta_{kb}) + v_x^2(\delta_{kc} + \delta_{kd}) + v_y^2(\delta_{ke} + \delta_{kf})$ |
| 3 | $v_x^4 + v_y^4 + v_z^4$ | $v_x v_y(\delta_{ka} - \delta_{kb}) + v_x v_z(\delta_{kc} - \delta_{kd}) + v_y v_z(\delta_{ke} - \delta_{kf})$ |
| 4 | $v^6$ | |
| 5 | $v^2(v_x^4 + v_y^4 + v_z^4)$ | |
| 6 | $v_x^2 v_y^2 v_z^2$ | |

* $k_i$ is unity on potato i, zero elsewhere.

TABLE IV

Expansion coefficients and percentage of completeness for the Fermi surface harmonic expansion of the density matrix coefficients of Nb. $T^{\alpha}_{J,S}$, $\nu^{\alpha}_{S}$, and $I_{\alpha}$ are given in dimensionless program units. To convert to atomic units multiply $\nu T^{\alpha}_{J,S}$ by $(2\pi/a)^2$, $\nu^{\alpha}_{S}$ by $(a/2\pi)^2$ and I by $(a/2\pi)^3$. a for Nb is 6.2294 a.u.

(a) Sheet 1 (Jack) $T^{\alpha}_{J,1}(\times\nu)$

| n | J | $00\Gamma_1$ | $11\Gamma_{15}$ | $22\Gamma_{25'}$ | $22\Gamma_{12}$ | $33\Gamma_{25}$ | $33\Gamma_{15}$ | $33\Gamma_{2'}$ | $13\Gamma_{15}$ |
|---|---|---|---|---|---|---|---|---|---|
| 0 | 0 | .000239 | .001673 | .050642 | .004502 | .003262 | .000537 | .000541 | -.000909 |
| 2 | 1 | .000092 | .001114 | -.008878 | .010720 | .002543 | .000287 | -.000048 | -.000551 |
| 4 | 2 | -.000095 | -.001038 | -.00027 | .001135 | -.000194 | -.000332 | -.000177 | .000569 |
| 4 | 3 | .000044 | .000127 | .001538 | -.002168 | -.000318 | .000108 | .000248 | -.000121 |
| 6 | 4 | -.000098 | .000020 | .000228 | -.000376 | .000015 | .000087 | .000178 | -.000097 |
| 6 | 5 | .000043 | .000230 | -.001353 | .001660 | .000361 | -.000017 | -.000222 | -.000047 |
| 6 | 6 | -.000047 | -.000096 | .000719 | -.000873 | -.000201 | -.000000 | .000034 | .000022 |
| $p^{\alpha}_{6,1}$ | | 67.4% | 97.3% | 99.9% | 99.1% | 99.5% | 96.0% | 91.1% | 96.6% |
| $\nu^{\alpha}_{1}$ | | .0007 | .0139 | 1.1854 | .0736 | .0284 | .0047 | .00009 | -.0025 |
| $I_{\alpha}$ | | 8.1707 | 23.552 | 66.200 | 46.222 | 24.647 | 24.529 | 4.666 | 7.690 |



TABLE IV (continued)

(b) Sheet 2 (Jungle Gym) $T^{\alpha}_{J,2}(\times\nu)$

| n | J | $00\Gamma_1$ | $11\Gamma_{15}$ | $22\Gamma_{25'}$ | $22\Gamma_{12}$ | $33\Gamma_{25}$ | $33\Gamma_{15}$ | $33\Gamma_{2'}$ | $13\Gamma_{15}$ |
|---|---|---|---|---|---|---|---|---|---|
| 0 | 0 | .009766 | .017143 | .086291 | .009875 | .005834 | .005202 | .008104 | -.005678 |
| 2 | 1 | .008841 | -.000225 | .000876 | -.003412 | -.002848 | .004249 | .004715 | -.003021 |
| 4 | 2 | .007407 | -.002116 | -.001656 | .001832 | .001379 | -.000309 | -.003000 | .000245 |
| 4 | 3 | -.001329 | -.001435 | .001474 | -.001054 | .000494 | -.000371 | -.000933 | -.000375 |
| 6 | 4 | -.000152 | .002832 | .000216 | -.001577 | -.000889 | .000265 | .001442 | .000234 |
| 6 | 5 | .001404 | .001130 | -.000546 | -.000049 | -.000482 | .000289 | .000533 | .000338 |
| 6 | 6 | -.001482 | -.000241 | .001267 | -.001184 | -.000027 | -.000440 | -.000075 | .000056 |
| $p^{\alpha}_{6,2}$ | | 94.6% | 90.2% | 99.7% | 88.0% | 97.1% | 99.0% | 95.3% | 98.3% |
| $\nu^{\alpha}_{2}$ | | .0529 | .2676 | 3.7856 | .3025 | .0953 | .0846 | .0251 | -.0289 |
| $I_{\alpha}$ | | 8.1707 | 23.552 | 66.200 | 46.222 | 24.647 | 24.529 | 4.666 | 7.690 |

TABLE IV (continued)

(c) Sheet (3) $T^{\alpha}_{J,3}(\times\nu)$

| n | J | $00\Gamma_1$ | $11\Gamma_{15}$ | $22\Gamma_{25'}$ | $22_{12}$ | $33\Gamma_{25}$ | $33\Gamma_{15}$ | $33\Gamma_{2'}$ | $13\Gamma_{15}$ |
|---|---|---|---|---|---|---|---|---|---|
| 0 | 0 | .057976 | .100722 | .029356 | .038861 | .007540 | .001321 | .002854 | .009696 |
| 2 | 1 | -.005141 | .001638 | -.006819 | .009288 | -.000522 | .000701 | -.000181 | .002865 |
| 2 | 2 | -.017362 | -.003379 | -.003942 | .010091 | .000061 | .000403 | -.000859 | .001120 |
| 2 | 3 | -.009829 | -.007728 | -.009658 | .018299 | .001763 | .000446 | -.001137 | .000882 |
| $p^{\alpha}_{2,3}$ | | 86.9% | 99.4% | 97.1% | 97.2% | 88.5% | 95.4% | 86.9% | 93.4% |
| $\nu^{\alpha}_3$ | | .3127 | 1.5661 | 1.2829 | 1.1858 | .1227 | .0214 | .0088 | .0492 |
| $I_{\alpha}$ | | 8.1707 | 23.552 | 66.200 | 46.222 | 24.647 | 24,529 | 4.6663 | 7.6900 |



Equation (86) implies that if a single function $T^{\alpha}(k)$ dominates the sum (86) for a particular sheet, then, T (k) must be approximately independent of k over this sheet and can be represented quite well by the FSH which is constant on that sheet. This circumstance obtains on the jack and jungle gym surfaces where the 22 $\Gamma_{25'}$ contribution dominates. Correspondingly we see that the expansion of $T_{22}{}^{\Gamma_{25'}}(k)$ is more than 99% complete for both of these surfaces taking only one FSH. Most of the other functions are also satisfactorily complete with the basis we have taken.

The few functions which are not well converged deserve closer scrutiny. The worst offender is the $00\Gamma_1$ function on the jack. Fortunately this contribution is of negligible magnitude ($\nu^{\alpha}_5/\nu < 0.0001$) and will not affect our calculation of $\lambda_{JJ'}$. These states are concentrated near the sharp cusp near the tips of the jack. The wave functions can be discontinuous in this region due to a band crossing in the $\Gamma$NH plane which would be removed by spin-orbit coupling (not included here). It is not yet clear whether the lack of convergence is due to unsuitability of the FSH's for describing this function or to numerical noise in the wavefunctions which are almost zero for these states.

The largest error in our estimation of the gap anisotropy and $T_c$ enhancement probably arises from the relatively poor convergence of the ($33\Gamma_{25}$) states on the potato. These states have a fairly high weight for f states and the coupling matrix $g_{\alpha\beta}$ is very large when $\alpha$ is a d state and $\beta$ is an f state. An examination of the distribution of the ($33\Gamma_{25}$) states over the potatoes does not reveal any pathological behavior and we speculate that only a few more polynomials of higher order than two will be required to complete the expansion. In any event our overall convergence is quite good as we shall show below.

## VIII. RESULTS AND COMPARISON WITH EXPERIMENT

Calculations of $\lambda$ for d-band metals based on reliable band structure information have only very recently been reported. Calculations of $\eta$ have been done for a number of metals[30-32], but the only detailed calculation of $\lambda$ for a transition element to our knowledge is that of Yamashita and Asano[35] for Nb and Mo. These authors use a very coarse mesh of points on the Fermi surface so that (in our opinion) the finer details of their results cannot be trusted. However, it is noteworthy that these authors have calculated the anisotropic function $\lambda_k$ as well as $\lambda$ for both elements. Extensive calculations of $\lambda_k$ and $\lambda$ have been reported for Cu by Nowak[36] and Das[37]. However, Cu has a much simpler Fermi surface than any true transition element. We report here the first calculation of the

anisotropy of $\Delta$ for any transition element. However, our calculations have not included the part of the anisotropy arising from the phonons. Our work is an extension to the anisotropic problem of previous calculations[30-32] of $\eta$.

The results of our calculation are two 18 × 18 real symmetric matrices, $\eta_{JJ'}$ and $H_{JJ'}$, calculated for Nb as described in previous sections. These matrices are then divided by $M\langle\omega^2\rangle = 5.527$ eV/Å$^2$ to yield the matrices $\lambda_{JJ'}$ and $\Lambda_{JJ'}$. There would be little point to presenting all 342 numbers-most of them are small at any rate. Instead we present the 18 numbers $\lambda_{0J}$ and the 18 numbers $\Delta_J$ in Table V. These coefficients can be used to construct the anisotropic mass renormalization $\lambda_k$ and gap $\Delta_k$. In the symmetric representation, all except the coefficients $\lambda_{00}$ and $\Delta_0$ are small. The calculated rms gap anisotropy $\alpha$ is 6%. Approximately half of this anisotropy is already obtained in a 3 × 3 calculation using only the constant polynomials - i.e. a 3 band model. The value of $\lambda$ is 1.27, in agreement with the calculation of ref.32. This value is significantly larger than the empirical[5] value of 0.82; probable reasons for the discrepancy are discussed in ref. 32. We believe that the electronic contribution to the relative anisotropy of $\lambda$ and $\Delta$ is correctly accounted for in our model even though an overall uncertainty in magnitude still exists. We obtained $\lambda_{eff}=0.51822$ which may be compared with the isotropic value $(\lambda-\mu^*)/(1+\lambda) = .51625$ yielding $\delta\lambda_{eff} = .00197$. This corresponds to a $T_c$ enhancement of 0.74% or 0.07°K. The matrix $\mu^*$ was taken to be $0.1\ \delta_{J0}\delta_{J'0}$ in the symmetric representation. These results are found by solution of the eigenvalue equation (26), and are in good agreement with the perturbative eq. (36). As a check on our calculations we have also calculated $\langle\lambda_k^2\rangle$ directly, without using the Fermi surface harmonic expansion. It is easy to verify that $\langle\lambda_k^2\rangle$ is given in our model by

$$\langle\lambda_k^2\rangle = (\nu/M\langle\omega^2\rangle)^2 \sum_{\alpha\beta}\sum_{\alpha'\beta'} T_0^{\alpha} T_0^{\alpha'} g_{\alpha\beta} g_{\alpha'\beta'} I_{\beta\beta'} \qquad (90)$$

where $I_{\beta\beta'}$ can either be expanded in FSH's or calculated directly,

$$I_{\beta\beta'} = \frac{1}{\nu}\sum_k \delta(\varepsilon_k)\, T^{\beta}(k)\, T^{\beta'}(k) = \sum_J T_J^{\beta} T_J^{\beta'} .$$

From direct calculation not using FSH's we obtain $\langle\lambda_k^2\rangle - \lambda^2 = .02307$ which compares very well with our eighteen term expansion $\sum_{J\neq 0}\lambda_{0J}^2 = .02271$. This gives us considerable extra confidence that the FSH basis set is complete.



It is somewhat disappointing to discover that the theoretically predicted anisotropy is so low. This is in accord with numerous experiments which we cite below. However, it violates an intuitive notion that Nb with its complicated non-spherical Fermi surface should be more anisotropic than a metal like Zn with a Fermi surface not too badly distorted from a sphere. Possibly d-band elements have an intrinsically more isotropic coupling constant than s-p-band elements, but if this is so, we do not yet understand why. To make the situation more confusing, the noble metals, which should occupy a middle ground, are known both from experiment[38,39] and theory[36,37] to have a relatively large anisotropy. Since the transition temperatures of the noble metals (if they in fact are finite) are very low, it seems likely that anisotropy enhancement will give a large increase in $T_c$ in these materials. This in turn suggests that sample purity may play a larger role than usually expected since impurity scattering strongly suppresses anisotropy enhancement[10-15] when $\hbar/\tau \gtrsim k_B T_c$.

The current experimental situation is not inconsistent with our theoretical estimate of 6% rms anisotropy of $\Delta$ in Nb. However, the experimental situation is far from unambiguous so we indulge here in a brief review. A variety of experiments, tunneling, ultrasonic attenuation, heat capacity, thermal conductivity, $T_c$ reduction in dilute alloys, and critical field anisotropy, can all be interpreted in terms of gap anisotropy. In niobium most of the experiments so far seem to have a somewhat ambiguous interpretation. Critical field anisotropy[40] is perhaps the least ambiguous experiment, but we have not yet made the kind of calculations which permit comparison. There are several sources of critical field anisotropy, some of which do not require $\Delta$ to be anisotropic. Williamson[40] measured a variation of 10% in $H_{c2}(\theta)$ as $\theta$ was varied in the $(1\bar{1}0)$ plane. This variation can be accounted for in a non-local model taking into account the known Fermi surface geometry and not necessarily requiring any anisotropy in $\Lambda$.

Heat capacity at low temperatures is most sensitive to the minimum energy gap, whereas nearer to $T_c$, a more nearly isotropic average of the gap is measured. Recent measurements of $C_V$ in Nb by Sellers et al[41] show no evidence for strong anisotropy and indicate that the anomalous results of earlier studies may have arisen from H impurities. A similar conclusion was reached by Anderson and collaborators in studies of the thermal conductivity[42,43].

The behavior of $T_c$ in dilute alloys of Nb has apparently not been much studied, although we may have missed some literature. The most systematic study known to us is by Ronami and Berezina[44] who found a sharp minimum in $T_c$ at concentrations less than 0.6% of column IV and VI transition metal impurities. Unfortunately they were unable to establish the precise concentration of the minimum because of sample difficulties, and they did not measure

TABLE V

Expansion coefficients for the energy gap and mass enhancement in Fermi Surface Harmonics. These coefficients are for the symmetric-orthonormal basis where $F_0$, $F_{0'}$ and $F_{0''}$ are symmetrized combinations of the functions which are constants on a single sheet.

| J | sheet | $\Delta_J/\Delta_0$ | $\lambda_{0J}$ |
|---|---|---|---|
| 0 | 1,2,3 | 1.0000 | 1.2739 |
| 0' | 1,2,3 | -.0390 | -.0883 |
| 0'' | 1,2,3 | -.0196 | -.0435 |
| 1 | 1 | .0273 | .0677 |
| 2 | 1 | -.0093 | -.0178 |
| 3 | 1 | .0007 | -.0016 |
| 4 | 1 | .0027 | .0045 |
| 5 | 1 | .0017 | .0062 |
| 6 | 1 | -.0016 | -.0045 |
| 1 | 2 | .0290 | .0821 |
| 2 | 2 | -.0043 | -.0073 |
| 3 | 2 | -.0010 | -.0037 |
| 4 | 2 | .0004 | .0005 |
| 5 | 2 | -.0008 | -.0015 |
| 6 | 2 | -.0034 | -.0101 |
| 1 | 3 | -.0107 | -.0227 |
| 2 | 3 | -.0080 | -.0169 |
| 3 | 3 | .0065 | .0181 |



the residual resistances. It is difficult to learn the magnitude of the depression at the minimum from their paper, but it is apparently around $0.2^oK$ and species dependent. We urge that further studies be made of this effect.

In principle the ideal experiment to probe gap anisotropy is single crystal tunneling, which can measure $\Delta$ in specific directions in $\hat{k}$ space. Also polycrystalline tunneling can determine the rms anisotropy from the broadening of the onset of normal resistance at $eV \sim \Delta$. Unfortunately the application of tunneling to transition elements has proved to be extremely difficult, probably because of surface contamination. A recent report[45] finds $2\Delta \sim 3.93kT_c$ in single crystal samples, with no evidence of any anisotropy greater than 2%. Earlier reports had been interpreted in terms of very large anisotropy, but this is now ascribed[45] to sample problems.

Ultrasonic attenuation has also been interpreted in terms of very large anisotropy, but recent experiments[46] on very pure samples are more consistent with an interpretation of very weak anisotropy. In the quantum regime $q\ell >> 1$ which is achieved only in very pure samples and high ultrasonic frequencies, the attenuation is caused by "belts" of electrons in the fermi surface with $v_{\hat{k}}$ perpendicular to the $\hat{q}$ of sound. At low temperatures the attenuation is principally caused by the states on this belt with the minimum gap. By analyzing low T attenuation data, Carsey et al[47] have found $2\Delta/k_BT_c = 3.7$ for $\hat{q}$ in the [111] direction, 3.64 in the [100] direction, and 3.84 in the [110] direction. A later experiment[48] with a purer sample and larger $q\ell$ revised the value on the [100] direction from 3.64 to 3.56. These experiments seem at the moment to provide the clearest evidence that rms gap anisotropy in Nb is in the range 5-10%. It is also noteworthy that a new technique which amounts to very high frequency ultrasonic attenuation has been developed using neutrons[49] and that within the resolution of this experiment, phonons in the [100] and [110] directions see the same energy gap in niobium.

At the moment it seems premature to make a very detailed comparison between theory and experiment. We can hope that in the near future both will improve and allow a more critical test of this interesting lapse in our microscopic understanding of d-band superconductors.

## ACKNOWLEDGEMENTS

P.B.A thanks R.C. Dynes for much instruction and stimulation in this field. W.H.B. thanks J.S. Faulkner and J.J. Olson for assistance in the development of KKR constant energy search and plotting routines.

## REFERENCES


1. J. Bardeen, L.N. Cooper and J.R. Schrieffer, Phys. Rev. 108, 1175 (1957).
2. G.M. Eliashberg, Zh. Eksp. Teor. Fiz. 38, 966 (1960); 39, 1437 (1960)[Sov. Phys. -JETP 11, 696 (1960); 12, 1000 (1961)].
3. D.J. Scalapino, J.R. Schrieffer, and J.W. Wilkins, Phys. Rev. 148, 263 (1966).
4. W.L. McMillan and J.M. Rowell, in Superconductivity, edited by R.D. Parks (Marcel Dekker, New York, 1969).
5. W.L. McMillan, Phys. Rev. 167, 331 (1968).
6. P.W. Anderson, J. Phys. Chem. Solids 11, 26 (1959); Proc. VII Int. Conf. on Low Temperature Physics, edited by G.M. Graham, Plenum, 1961, p. 298.
7. H. Suhl, B.T. Matthias, and L.R. Walker, Phys. Rev. Lett. 3, 552 (1959).
8. V.A. Moskalenko, Fiz. Met. Metalloved. 8, 503 (1959).
9. V.L. Pokrovskii, Zh. Eksp. Teor. Fiz. 40, 641 (1961). [Sov. Phys. - JETP 13, 447 (1961)].
10. D. Markowitz and L.P. Kadanoff, Phys. Rev. 131, 563 (1963).
11. T. Tsuneto, Prog. Theor. Phys. 28, 857 (1962).
12. C. Caroli, P.G. DeGennes, and J. Matricon, J. Phys. Rad. 23, 707 (1962).
13. P. Hohenberg, Zh. Eksp. Teor. Fiz. 45, 1208 (1963); [Sov. Phys. - JETP 18, 834 (1964)].
14. D.M. Brink and M.J. Zuckermann, Proc. Phys. Soc. (London) 85, 329 (1965).
15. J.R. Clem, Phys. Rev. 148, 392 (1966).
16. H. Teichler, Phil. Mag. 31, 775 (1975), and references therein.
17. P. Entel and M. Peter, J. Low. Temp. Phys. 22, 613 (1976).
18. P.B. Allen, Bull. Am. Phys. Soc. Ser. II, 21, 259 (1976).
19. P.B. Allen, Bull. Am. Phys. Soc. Ser. II, 21, 102 (1976).
20. P.B. Allen, Phys. Rev. B13, 1416 (1976).
21. P.B. Allen and R.C. Dynes, Phys. Rev. B12, 905 (1975).
22. P.B. Allen, Sol. State Commun. 14, 937 (1974).
23. J. Appel and H. Heyszenau, Phys. Rev. 188, 755 (1969); I. Foulkes and B.L. Gyorffy, preprint.
24. P.W. Anderson and P. Morel, Physica (Utr.) 26, 671 (1960), Phys. Rev. 123, 1911 (1961).
25. C.R. Leavens and J.P. Carbotte, Ann. Phys. (N.Y.) 70, 338 (1972).
26. D. Farrell, J.G. Park and B.R. Coles, Phys. Rev. Lett. 13, 328 (1964).
27. B.T. Geilikman and N.F. Masharov, Fiz. Met. Metalloved, 32, 492 (1971). B.T. Geilikmann, R.O. Zaitsev, and V.Z. Kresin, Fiz. Trend. Tela. (1967)[Sov. Phys. - Solid State 9, 642 (1967)].
28. L.P. Bouchaert, R. Smoluchowski, and E. Wigner, Phys. Rev. 50, 58 (1936).
29. J.J. Hopfield, Phys. Rev. 186, 443 (1969).
30. G.D. Gaspari and B.L. Gyorffy, Phys. Rev. Lett. 28, 801 (1972).





31. B.M. Klein and D.A. Papaconstantopoulos, Phys. Rev. Lett. 32, 1193 (1974).
32. W.H. Butler, J.J. Olson, J.S. Faulkner, and B.L. Gyorffy, Phys. Rev. B (in press).
33. J.S. Faulkner, H.L. Davis, and H.W. Joy, Phys.Rev. 161, 656 (1967).
34. L.F. Mattheiss, Phys. Rev. B1, 373 (1970).
35. J. Yamashita and S. Asano, Prog. Theor. Phys. 51, 317 (1974).
36. D. Nowak, Phys. Rev. B6, 3691 (1972).
37. S.G. Das, Phys. Rev. B7, 2238 (1973).
38. M.J.G. Lee, Phys. Rev. B2, 250 (1970).
39. N.E. Christensen, Sol. State Commun. 9, 749 (1971).
40. S.J. Williamson, Phys. Rev. B2, 3545 (1970).
41. G.J. Sellers, A.C. Anderson, and H.K. Birnbaum, Phys. Rev. B10, 2771 (1974).
42. A.C. Anderson, C.B. Satterthwaite, and S.C. Smith, Phys. Rev. B3, 3762 (1971).
43. S.G. O'Hara, G.J. Sellers and A.C. Anderson, Phys. Rev. B10, 2777 (1974).
44. G.N. Ronami and V.P. Berezina, Fiz. Met. Metalloved. 37, 872 (1974).
45. J.Bostock, K. Agyeman, M.H. Frommer and M.L.A. MacVicar, J. Appl. Phys. 44, 5567 (1973).
46. D.P. Almond, M.J. Lea and E.R. Dobbs, Phys. Rev. Lett. 29, 764 (1972).
47. F. Carsey, R. Kagiwada, M. Levy and K. Maki, Phys. Rev. B3, 854 (1971).
48. F. Carsey and M. Levy, Phys. Rev. B7, 4123 (1973).
49. S.M. Shapiro, G. Shirane, and J.D. Axe, Phys. Rev. B12, 4899 (1975).


## QUESTIONS AND COMMENTS

E. Fawcett: This is a Fermi surface question. You have shown drawings of the Fermi surface of Nb which do not seem to agree with my recollection of the Fermi surface given by Mattheiss' calculation.

W. Butler: The Fermi surface which we obtained is essentially the same as Mattheiss. I think you recognize the distorted ellipsoid, and you recognize the jack. The third sheet which we have shown as a surface containing electrons centered at P will look quite different if it is drawn as a surface containing holes centered at Γ.

B. Gyorffy: Can you tell if there were any cancellations? The final result might come out small, but if there were cancellations during the calculation one should conclude that this is not a general rule and, indeed, in other

systems you might have a bigger anisotropy.

W. Butler: Yes, there were cancellations. The small value of the gap anisotropy is due not only to the fact that the density matrix expansion coefficients $T_J^\alpha$ are small in absolute value for $J \neq 0$, but also to the fact that they can be positive or negative. I would guess that the rms anisotropy might be doubled or tripled if one were to replace the $T_J^\alpha$'s by their absolute values in calculating the gap. Other systems would be expected to have "cancellations" too, however, and it is not clear that niobium is an exceptional system with regard to the importance of this effect.

J. Phillips: This is a cubic crystal. The example you took before is zinc which is hexagonal. Do you expect much bigger anisotropy?

W. Butler: Generally we expect bigger anisotropy in hexagonal systems than in cubic. Zinc, however, is generally considered to be a simple metal with a Fermi surface not too much distorted from a sphere. Our initial expectation was that the complicated Fermi surfaces of transition metals should lead to large anisotropies compared to the simple metals.

J. Bostock: You get a mean square anisotropy of 0.004 which is presumably what your approximation allows you to calculate to some accuracy. What is that accuracy?

W. Butler: There are various sources of error. The most important source is our neglect of anisotropy arising from the phonons. Our initial expectation was that the electronic contribution to the gap anisotropy would be at least as important as the phonon contribution. Now that the electronic contribution has turned out to be so small we can no longer be confident that this is so. We plan to treat the phonons on an equal footing with the electrons in a later calculation. As for the other sources of error---Fermi surface harmonic expansion convergence, band theory convergence, matrix element uncertainties, etc.---we estimate the net effect of these errors on the relative gap anisotropy to be on the order of 10%.

F. Mueller: Would you care to speculate on the anisotropies in the A-15's---in terms of similar kinds of calculations?

W. Butler: No. Except to say that our calculation for Nb indicates



that one can have a very anisotropic Fermi surface which does not lead to a large anisotropy of the gap function. This is partly due to the fact that in Nb the density of states is fairly uniformly distributed over the Fermi surface. This might happen in the A-15's also.

F. Mueller: Do you think the anisotropy in the A-15's is larger, for example?

W. Butler: You obviously have a very strange Fermi surface there. A very anisotropic Fermi surface.

F. Mueller: We are not talking about doing real calculations. We all know that they are very difficult.

W. Butler: The only thing I am going to say, Fred [Mueller], is how I use my intuition here. I say 'well, I see a very anisotropic Fermi surface and maybe there is a big anisotropy in the gap. There is a big anisotropy in the Fermi surface obviously of niobium and it did not lead to such a big anisotropy of the gap'.

R. Dynes: I think the point is that niobium is a surprise.

W. Butler: Yes, that is all I am saying.

F. Mueller: I did not find niobium so surprising.

W. Butler: You have better intuition, that's all.

C. Varma: It is quite possible, the fact that the gap function involves a convolution integral over the Fermi surface implies that anisotropy in the Fermi surface will not reflect equally in the gap function. I have a different question. There are several weak-coupling calculations in the literature that suggest that if the mean free path due to impurity scattering is less than the coherence length, the gap will be isotropic. Are there reasons to believe that this result will not hold in a strong-coupling calculation?

W. Butler: No. Our calculation, however, neglected impurity scattering. It should be applicable in the limit of very long mean free path.

P. Allen: It is true that the anisotropy enhancement of $T_c$ is diminished when the mean free path ($\ell$) is as short as the coherence length ($\xi$). However, the enhancement by no means vanishes at that point. It washes out

rather slowly and continues to be measureable even when $\ell$ is much shorter than $\xi$.

J. Bostock: One more experimental comment: If you look at ultrasonic data, or thermal conductivity, or specific heat there is zero anisotropy observed for niobium.

W. Butler: I thought it was more than zero.

J. Bostock: Zero.

P. Allen: Ultrasonic attenuation measurements by Carsey et al. [Refs. 47 and 48] suggest 5 or 10% anisotropy.

J. Bostock: That is not al all clear; see C. Gough's paper.

M. Strongin: I am a little confused about Varma's remarks because in niobium if I remember the coherence length is something like 400 Å and at room temperature the mean free path is something like 50 Å, but if you have a resistance ratio of 100 then the mean free path at low temperatures would be much larger than the coherence length.

C. Varma: I am talking about the impurity mean free path and I am really concerned about the A-15's.

W. Butler: That depends on how pure you get your niobium, doesn't it?

B. Klein: We know that anisotropies in k space are just something like Fourier transforms of anisotropies in real space. Since it is well known from the band structure point of view that using spherically averaged charge densities and potentials give very good values of macroscopic quantities, maybe it isn't such a surprise that anisotropies in k space do not show up very strongly.